

Reference Correlation of the Thermal Conductivity of Carbon Dioxide from the Triple Point to 1100 K and up to 200 MPa

F EP

Cite as: J. Phys. Chem. Ref. Data **45**, 013102 (2016); <https://doi.org/10.1063/1.4940892>

Submitted: 28 April 2015 . Accepted: 13 January 2016 . Published Online: 25 February 2016

M. L. Huber, E. A. Sykioti, M. J. Assael, and R. A. Perkins

COLLECTIONS

F This paper was selected as Featured

EP This paper was selected as an Editor's Pick



View Online



Export Citation



CrossMark

ARTICLES YOU MAY BE INTERESTED IN

Reference Correlation for the Viscosity of Carbon Dioxide

Journal of Physical and Chemical Reference Data **46**, 013107 (2017); <https://doi.org/10.1063/1.4977429>

A New Equation of State for Carbon Dioxide Covering the Fluid Region from the Triple-Point Temperature to 1100 K at Pressures up to 800 MPa

Journal of Physical and Chemical Reference Data **25**, 1509 (1996); <https://doi.org/10.1063/1.555991>

New Formulation for the Viscosity of Propane

Journal of Physical and Chemical Reference Data **45**, 043103 (2016); <https://doi.org/10.1063/1.4966928>

Where in the **world** is AIP Publishing?
Find out where we are exhibiting next



Reference Correlation of the Thermal Conductivity of Carbon Dioxide from the Triple Point to 1100 K and up to 200 MPa

M. L. Huber^{a)}

Applied Chemicals and Materials Division, National Institute of Standards and Technology, 325 Broadway, Boulder, Colorado 80305, USA

E. A. Sykioti and M. J. Assael

Laboratory of Thermophysical Properties and Environmental Processes, Chemical Engineering Department, Aristotle University, Thessaloniki 54636, Greece

R. A. Perkins

Applied Chemicals and Materials Division, National Institute of Standards and Technology, 325 Broadway, Boulder, Colorado 80305, USA

(Received 28 April 2015; accepted 13 January 2016; published online 25 February 2016)

This paper contains new, representative reference equations for the thermal conductivity of carbon dioxide. The equations are based in part upon a body of experimental data that has been critically assessed for internal consistency and for agreement with theory whenever possible. In the case of the dilute-gas thermal conductivity, we incorporated recent theoretical calculations to extend the temperature range of the experimental data. Moreover, in the critical region, the experimentally observed enhancement of the thermal conductivity is well represented by theoretically based equations containing just one adjustable parameter. The correlation is applicable for the temperature range from the triple point to 1100 K and pressures up to 200 MPa. The overall uncertainty (at the 95% confidence level) of the proposed correlation varies depending on the state point from a low of 1% at very low pressures below 0.1 MPa between 300 and 700 K, to 5% at the higher pressures of the range of validity. © 2016 by the U.S. Secretary of Commerce on behalf of the United States. All rights reserved. [<http://dx.doi.org/10.1063/1.4940892>]

Key words: carbon dioxide; critical phenomena; thermal conductivity; transport properties.

CONTENTS

1. Introduction.....	2	6. Conclusion.....	16
2. Methodology.....	3	Acknowledgments.....	16
3. The Correlation.....	3	7. References.....	16
3.1. The dilute-gas limit.....	6		
3.2. The residual thermal conductivity.....	8		
3.3. The critical enhancement.....	8		
3.3.1. Simplified crossover model.....	8		
3.3.2. Thermal diffusivity validation.....	11		
3.3.3. Empirical critical enhancement.....	13		
4. Uncertainty Assessments.....	13		
4.1. Uncertainty outside of the critical region....	13		
4.2. Uncertainty in the critical region.....	14		
5. Computer-Program Verification and Recommended Values.....	15		

List of Tables

1. Thermal-conductivity measurements of carbon dioxide.....	4
2. Primary data considered for dilute-gas analysis ..	7
3. Coefficients in Eq. (3) for λ_0	8
4. Coefficients of Eq. (4) for the residual thermal conductivity of carbon dioxide.....	8
5. Evaluation of the carbon dioxide thermal-conductivity correlation for the primary data.....	8
6. Evaluation of the carbon dioxide thermal-conductivity correlation for all data sets.....	9
7. Sample points for computer verification of the correlating equations.....	15
8. Recommended values of CO ₂ thermal conductivity (mW m ⁻¹ K ⁻¹).....	15

^{a)}Author to whom correspondence should be addressed; electronic mail: marcia.huber@nist.gov.

© 2016 by the U.S. Secretary of Commerce on behalf of the United States. All rights reserved.

List of Figures

1. Temperature and pressure ranges of the primary experimental thermal-conductivity data for carbon dioxide.	6	15. Thermal diffusivity of CO ₂ along the critical isochore close to the critical temperature from the Rayleigh scattering line width from Swinney and Henry ¹²⁸ (Δ) and the transient interferometry measurements of Becker and Grigull ⁵² (\bullet).	13
2. Dataset for λ_0 used in the regression.	7	16. Thermal conductivity along isotherms near the critical point measured directly by Michels <i>et al.</i> ³⁹ and calculated from the thermal diffusivity data of Becker and Grigull ⁵² with ρ and C_p from the Albright <i>et al.</i> equation of state. ¹²⁷	13
3. Comparison of λ_0 correlations with the theoretical and experimental data.	7	17. Percentage deviations of all primary experimental data of carbon dioxide from the values calculated by the full model Eqs. (1) and (3)–(8) as a function of temperature.	14
4. Percentage deviations of primary experimental data of carbon dioxide from the values calculated by the present model as a function of temperature, for the vapor region.	10	18. Percentage deviations of all primary experimental data of carbon dioxide from the values calculated by the empirical critical enhancement model Eqs. (1), (3), (4), and (10) as a function of temperature.	14
5. Percentage deviations of primary experimental data of carbon dioxide from the values calculated by the present model as a function of pressure, for the vapor region.	10	19. Estimated uncertainty for the correlation excluding the critical region.	14
6. Percentage deviations of primary experimental data of carbon dioxide from the values calculated by the present model as a function of temperature, for the supercritical region at temperatures to 500 K.	10	20. Deviations in λ for the present correlation with thermodynamic properties calculated with the equation of state of Span and Wagner ¹¹⁴ relative to the Albright <i>et al.</i> ¹²⁷ scaled equation of state in the critical region.	14
7. Percentage deviations of primary experimental data of carbon dioxide from the values calculated by the present model as a function of pressure, for the supercritical region at temperatures to 500 K.	11	21. Deviations in a for the present correlation with thermodynamic properties calculated with the equation of state of Span and Wagner ¹¹⁴ relative to the Albright <i>et al.</i> ¹²⁷ scaled equation of state in the critical region.	14
8. Percentage deviations of primary experimental data of carbon dioxide from the values calculated by the present model as a function of temperature, for the supercritical region at temperatures above 500 K.	11	22. Deviations in λ and a for the present correlation with thermodynamic properties calculated with the equation of state of Span and Wagner ¹¹⁴ relative to the Albright <i>et al.</i> ¹²⁷ scaled equation of state near the critical temperature, along the critical isochore.	15
9. Percentage deviations of primary experimental data of carbon dioxide from the values calculated by the present model as a function of pressure, for the supercritical region at temperatures above 500 K.	11	23. Thermal conductivity of CO ₂ as a function of temperature for different pressures.	16
10. Percentage deviations of primary experimental data of carbon dioxide from the values calculated by the present model as a function of temperature, for the liquid phase.	11	24. Thermal-conductivity surface of CO ₂	16
11. Percentage deviations of primary experimental data of carbon dioxide from the values calculated by the present model as a function of pressure, for the liquid phase.	12		
12. Percentage deviations of primary experimental data of carbon dioxide from the values calculated by the Vesovic <i>et al.</i> ⁵ model as a function of temperature, for the liquid phase.	12		
13. Percentage deviations of primary experimental data of carbon dioxide from the values calculated by the Scalabrin <i>et al.</i> ⁶ model as a function of temperature, for the liquid phase.	12		
14. Thermal diffusivity of CO ₂ measured with interferometry of the fluid sample below a transient heated plate by Becker and Grigull ⁵² along isotherms near the critical point.	12		

1. Introduction

Carbon dioxide is a widely used industrial fluid with many applications including as a solvent for supercritical extraction,¹ as a refrigerant,² to aid in enhanced oil recovery,³ and most recently as a potential working fluid in supercritical Brayton cycles that may be used in solar, geothermal, or other power cycle applications.⁴ It is, therefore, important to have available accurate formulations for the thermodynamic and transport properties of this fluid.

In 1990, Vesovic *et al.*⁵ published a reference correlation for the thermal conductivity surface of carbon dioxide valid over the temperature range from 200 to 1000 K and up to 100 MPa. In 2006, Scalabrin *et al.*⁶ developed a new correlation that extended the upper pressure limit to 200 MPa. The uncertainty of both of these formulations, however, is limited due to the

data available at the time. Recently, new measurements have been made⁷ that allow improvements in the uncertainty of a CO₂ thermal conductivity correlation, especially in the liquid phase. In addition, there have been recent improvements in the potential energy surface that provide values for the thermal conductivity in the dilute-gas limit⁸ that can be used to guide the behavior of the dilute gas, especially at low and high temperatures where quality data are scarce or unavailable. The present work aims to incorporate both new data and theory to provide an improved wide-ranging correlation for the thermal conductivity of carbon dioxide that is valid over gas, liquid, and supercritical states.

In a series of recent papers, reference correlations for the thermal conductivity of normal and parahydrogen,⁹ SF₆,¹⁰ toluene,¹¹ benzene,¹² xylenes and ethylbenzene,¹³ *n*-hexane,¹⁴ *n*-heptane,¹⁵ methanol,¹⁶ ethanol,¹⁷ and water,¹⁸ as well as a series of reference correlations for the viscosity of fluids,^{19–22} covering a wide range of conditions of temperature and pressure, were reported. In this paper, the work is extended to the thermal conductivity of carbon dioxide.

2. Methodology

The thermal conductivity λ is expressed as the sum of three independent contributions as

$$\lambda(\rho, T) = \lambda_o(T) + \Delta\lambda(\rho, T) + \Delta\lambda_c(\rho, T), \quad (1)$$

where ρ is the density, T is the temperature, and the first term, $\lambda_o(T) = \lambda(0, T)$, is the contribution to the thermal conductivity in the dilute-gas limit, where only two-body molecular interactions occur. The final term, $\Delta\lambda_c(\rho, T)$, the critical enhancement, arises from the long-range density fluctuations that occur in a fluid near its critical point, which contribute to divergence of the thermal conductivity at the critical point. Finally, the term $\Delta\lambda(\rho, T)$, the residual property, represents the contribution of all other effects to the thermal conductivity of the fluid at elevated densities, including many-body collisions, molecular-velocity correlations, and collisional transfer.

The identification of these three separate contributions to the thermal conductivity and to transport properties in general is useful because it is possible, to some extent, to treat both $\lambda_o(T)$ and $\Delta\lambda_c(\rho, T)$ theoretically. In addition, it is possible to derive information about $\lambda_o(T)$ from experiment. In contrast, there is almost no theoretical guidance concerning the residual contribution, $\Delta\lambda(\rho, T)$, so that its evaluation is based entirely on experimentally obtained data.

The analysis described above should be applied to the best available experimental data for the thermal conductivity. Thus, a prerequisite to the analysis is a critical assessment of the experimental data. For this purpose, two categories of experimental data are defined: primary data employed in the development of the correlation, and secondary data used simply for comparison purposes. According to the recommendation adopted by the Subcommittee on Transport Properties (now known as The International Association for Transport Properties) of the International Union of Pure and Applied Chemistry, the primary data are identified by

a well-established set of criteria.²³ These criteria have been successfully employed to establish standard reference values for the viscosity and thermal conductivity of fluids over wide ranges of conditions, with uncertainties in the range of 1%. However, in many cases, such a narrow definition unacceptably limits the range of the data representation. Consequently, within the primary data set, it is also necessary to include results that extend over a wide range of conditions, albeit with a poorer accuracy, provided they are consistent with other more accurate data or with theory. In all cases, the accuracy claimed for the final recommended data must reflect the estimated uncertainty in the primary information.

3. The Correlation

Table 1 summarizes, to the best of our knowledge, the experimental measurements^{7,24–112} of the thermal conductivity of carbon dioxide reported in the literature. Eighty nine one sets are included in the table. From these sets, 21 were considered as primary data. We started with the same data sets that were considered as primary in the work of Vesovic *et al.*⁵ in Tables 2 and 7 of Ref. 5. This includes the work of Millat *et al.*,²⁵ Johns *et al.*,²⁶ Clifford *et al.*,²⁹ Scott *et al.*,²⁸ Bakulin *et al.*,³³ Keyes,⁴¹ Lenoir and Comings,⁴² Johnston and Grilly,⁴³ Dickins,⁴⁴ Snel *et al.*,³⁰ and LeNeindre *et al.*^{35–38} Initially, we considered the single point of Franck⁸⁹ at 197 K that was considered primary in Vesovic *et al.*,⁵ but it was later not used as discussed in Sec. 3.1. For Millat *et al.*,²⁵ following Vesovic *et al.*,⁵ we also did not select any data from the 425 K isotherm. We included all points of Johns *et al.*²⁶ (except for one at a nominal temperature of 430 K and 20.4 MPa which is anomalously lower than others at that isotherm). All points from Clifford *et al.*,²⁹ Dickins,⁴⁴ Johnston and Grilly,⁴³ and Snel *et al.*³⁰ were included in the primary set. Following Vesovic, we also excluded the 316 K isotherm from Scott *et al.*²⁸ from the primary set. Initially, all points in Keyes⁴¹ were included in the primary set, but two points at the highest pressures at 273 K were later excluded. In addition, we added to the primary set the data from Keyes⁴⁰ as they extended down to 207 K. From Lenoir and Comings,⁴² we included only the points at atmospheric pressure as the density dependence of the other data in this set was inconsistent with other data. All points from the data of Bakulin *et al.*,³³ made with a steady-state hot-wire apparatus, were included in the primary set. In addition, we added another set of Bakulin's measurements³² to the primary set, but excluded data above 1000 K, as we rely on the theoretical calculations of Hellmann⁸ in this region as will be discussed below. We also included the data of LeNeindre *et al.*^{35–38} in the primary data set. All data from LeNeindre's work were included, including the highest temperature data extending to 951 K, with the exception of several points that appeared to have typographical errors or that were clearly inconsistent with other data. This included one point from Ref. 37 at 298 K, 30 MPa, and 3 points at 366 K and 70.3 MPa, at 372.45 K and 41.6 MPa, and 529 K, 35.2 MPa, from Ref. 35.

Although not considered primary in Vesovic's analysis,⁵ we included all measurements of Haarman³⁴ and those of Imaishi

TABLE 1. Thermal-conductivity measurements of carbon dioxide

First author	Year of publication	Technique employed ^a	Purity (%)	Uncertainty (%)	No. of data	Temperature range (K)	Pressure range (MPa)
Primary data							
Perkins ^{7,b}	2016	THW,SSHWS	99.994	0.5–3	4824	218–757	0.1–68.7
Li ²⁴	1994	THW	99.999	1.6	14	324	0.19–2.1
Millat ^{25,b}	1987	THW	99.995	1	91	305–425	0.68–6.7
Johns ²⁶	1986	THW	99.995	1	46	380–474	1.83–30.6
Imaishi ²⁷	1984	THW	99.9	0.5	23	300–301	0.62–3.9
Scott ^{28,b}	1983	THW	99.995	1	92	301–349	0.3–24.6
Clifford ²⁹	1979	THW	99.999	0.5	22	301–304	0.6–5.9
Snel ³⁰	1979	HW	99.99	1	133	298–323	0.004–5.5
Tarzmanov ^{31,b}	1978	SSHWS,CC	99.9	3	94	292–678	0.1–196
Bakulin ^{32,b}	1976	HF	na	5	10	400–1300	0.015
Bakulin ³³	1975	HF	na	5	28	225–316	0.1–2
Haarman ³⁴	1973	THW	na	1	8	328–468	0.1
Le Neindre ^{35,36}	1973	CC	na	2–5	536	293–961	0.1–128
LeNeindre ^{37,b}	1972	CC	na	2–5	194	298–951	0.1–120
Le Neindre ^{38,b}	1968	CC	na	2–5	31	294–309	0.1–104
Michels ^{39,b}	1962	PP	na	2	253	298–322	0.1–18
Keyes ⁴⁰	1955	CC	na	5	2	207–273	0.1
Keyes ⁴¹	1951	CC	na	5	9	273–423	0.1–6
Lenoir ^{42,b}	1951	CC	99.5	2	32	314–340	0.1–20.7
Johnston ^{43,b}	1946	HW	99.999	1–5	14	186–379	0.001
Dickins ⁴⁴	1934	HW	na	1	6	285	0.0001–0.001
Secondary data							
Tomida ⁴⁵	2010	THW	na	3	19	273–294	4–15
Patek ⁴⁶	2005	THW	99.98	1.2	77	298–428	0.5–15
Heinemann ⁴⁷	2000	THW	na	5	3	323–420	0.1
Chen ⁴⁸	1999	TM	na	2	66	304–316	1.5–13
Dohm ⁴⁹	1999	THW	na	5	7	300–420	0.1
Zheng ⁵⁰	1984	CC	99.5	3	13	298	0.10–5.4
Yorizane ⁵¹	1983	CC	99.0	3	15	303–323	0.1–4.5
Becker ^{52,c}	1978	HolInt	99.994	3–5	216	298–308	3–49
Ulybin ⁵³	1977	HW	na	5	14	225–312	0.112–1.01
Chen ⁵⁴	1975	TEM	99.995	5	34	350–2000	0.1
Salmanov ⁵⁵	1973	SSHWS	99.9	3	19	222–282	2–9
Shashkov ⁵⁶	1973	SSHWS	na	4	9	315–403	0.1
Dijkema ⁵⁷	1972	CC	na	na	2	298–333	0.1
Gupta ⁵⁸	1970	HW	na	5	11	373–1348	0.07
Maczek ⁵⁹	1970	SSHWS	na	3	1	323	0.1
Murthy ⁶⁰	1970	PP	99.99	3	53	305–310	7.5–8.3
Murthy ⁶¹	1970	PP	99.99	3	3	305–307	0.1–8.2
Tarzmanov ⁶²	1970	SSHWS	99.9	3	52	299–678	0.1–98.1
Golubev ⁶³	1969	CC	na	1.5–3	733	180–1400	0.1–51.0
Rosenbaum ⁶⁴	1969	CC	na	3	50	335–434	3–69
Barua ⁶⁵	1968	HW	99.5	1	5	283–473	0.1
Shingarev ⁶⁶	1968	SSHWS	na	na	23	231–326	1–19.6
van Dael ⁶⁷	1968	HW	99.95	0.5	1	296	0.1
Freud ⁶⁸	1967	TEM	99.9	10	42	298	0.48–56
Mukhopadhyay ⁶⁹	1967	HW	na	1	7	258–473	0.1
Mukhopadhyay ⁷⁰	1967	HW	na	2	5	273–473	0.1
Baker ⁷¹	1964	HW	na	na	1	478	0.1
Senftleben ⁷²	1964	na	na	4	8	273–673	0.1
Amirkhanov ⁷³	1963	PP	99.96	1	20	293–304	5.7–7.2
Cheung ⁷⁴	1962	CC	na	5	2	376–593	0.1
Guildner ⁷⁵	1962	CC	99.5	5	39	277–348	0.21–30
Westenberg ⁷⁶	1962	TWHWS	na	3	3	299–500	0.1
Geier ⁷⁷	1961	CC	na	2	23	273–1273	0.1
Vines ⁷⁸	1960	CC	na	1	4	543–1174	0.1
Chaikin ⁷⁹	1958	HW	na	10	5	293–503	0.1
Guildner ⁸⁰	1958	CC	99.99	5	22	304–348	0.2–30.4
Waelbroeck ⁸¹	1958	HW	na	na	1	313	0.1
Salceanu ⁸²	1956	HW	na	na	1	303	0.05
Kulakov ⁸³	1955	HW	na	na	2	338, 603	0.1
Rothman ⁸⁴	1955	CC	99.5	1	2	651–842	0.099–0.100
Filippov ⁸⁵	1954	HW	na	3	6	288–363	0.1

TABLE 1. Thermal-conductivity measurements of carbon dioxide—Continued

First author	Year of publication	Technique employed ^a	Purity (%)	Uncertainty (%)	No. of data	Temperature range (K)	Pressure range (MPa)
Thomas ⁸⁶	1954	SSHW	na	0.04–0.2	4	313–337	0
Davidson ⁸⁷	1953	CC	na	5	1	273	0.1
Rothman ⁸⁸	1953	CC	99.5	7.5	25	631–1047	0.1
Franck ⁸⁹	1951	HW	na	na	7	197–598	0.02–0.04
Kannuiluik ⁹⁰	1950	HW	na	0.3	9	275	0.001–0.11
Stolyarov ⁹¹	1950	HW	99	3	17	280–475	0.1–30
Borovik ⁹²	1949	HW	na	na	18	283–313	5.1–9.1
Keyes ⁹³	1949	CC	na	5	8	223–623	0.1
Stops ⁹⁴	1949	HW	na	na	1	273	0.1
Timrot ⁹⁵	1949	HW	99.0	4	160	293–473	0.1–29
Kannuiluik ⁹⁶	1947	HW	na	5	26	196–373	0.1
Vargaftik ⁹⁷	1946	HW	na	na	13	325–881	0.1
Eucken ⁹⁸	1940	HW	na	na	6	195–598	0.1
Koch ⁹⁹	1940	na	na	5	71	283–313	0.1–9
Sherratt ¹⁰⁰	1939	HW	na	na	10	339–565	0.1
Archer ¹⁰¹	1935	HW	na	0.4	11	285–591	0.1
Kannuiluik ¹⁰²	1934	HW	na	2	1	273	0.1
Kardos ¹⁰³	1934	na	na	na	6	273–308	5.9–8.8
Sellschopp ¹⁰⁴	1934	HW	na	2.5	50	284–323	0.10–9.15
Trautz ¹⁰⁵	1933	HW	na	1	19	273	0.24–1.19
Kornfeld ¹⁰⁶	1931	HW	na	na	1	298	0.1
Gregory ¹⁰⁷	1927	HW	99.82	na	6	278–286	0.1
Weber ¹⁰⁸	1927	HW	na	1	1	273	0.1
Weber ¹⁰⁹	1917	HW	na	na	1	273	0.1
Schleiermacher ¹¹⁰	1888	HW	na	na	1	298	0.1
Graetz ¹¹¹	1881	HW	na	na	1	273	0.1
Winkelmann ¹¹²	1880	HW	na	na	1	298	0.1

^aCC, coaxial cylinder; HF, hot filament; HolInt, heated plate observed by holographic interferometry; HW, hot wire; na, not available; PP, parallel plate; SSHW, steady-state hot wire; TEM, thermoelectric method; THW, transient hot wire; TWHW, thermal wake following hot-wire heating.

^bOnly selected points considered primary.

^cThermal diffusivity.

*et al.*²⁷ as primary data. Haarman's measurements³⁴ were made in a transient hot-wire apparatus and cover 328 to 468 K at atmospheric pressure. Imaishi *et al.*²⁷ were also transient hot-wire measurements but cover a very small temperature region around 301 K at pressures to 4 MPa. Finally, sources of primary data that focus on the critical region³⁹ were included, although in the development of the background equation points within 1 K of critical were not used. Michels *et al.*³⁹ measured the thermal conductivity in the critical region with a parallel plate apparatus, and in addition to points within 1 K of critical we also excluded some points near the coexistence line (298 K, 6.4249 MPa; 298 K, 6.4208–6.4338 MPa; 303 K, 7.202–7.209 MPa) and any points that were marked with an asterisk in their tables. The thermal diffusivity data of Becker and Grigull⁵² were only used for analysis and validation of the critical region and were not used in the development of the background function, and will be discussed further in Sec. 3.3.

Surprisingly, since Vesovic *et al.*⁵ made their correlation in 1990, very few new measurements have been made.^{7,24,45–49} The only new measurements suitable as primary data are those of Li *et al.*²⁴ and the very recent work of Perkins.⁷ Li's work was done with a transient hot-wire instrument with an estimated uncertainty of 1.6% but is limited to one isotherm at 324 K; all of these points were included in the primary data set. The measurements of Perkins⁷ were obtained with two hot-wire instruments: a low-temperature apparatus (218–340 K) and a high-temperature apparatus (300–750 K)

at pressures up to 70 MPa. Both steady-state and transient hot-wire measurements were made, with uncertainties ranging from a low of 0.5% for the liquid, increasing to 3% for gas below 1 MPa, for temperatures above 500 K, and in the critical region. The data set of Perkins⁷ is large compared to the others, and not all points from Perkins were used as primary data. We included in the primary set the data measured with double platinum hot wires, but for points measured with a single platinum wire included only those where the temperature ranges did not overlap since the double-wire data were considered of lower uncertainty and were preferred for primary data. We also did not include transient data from Perkins⁷ for low-density gas at temperatures above 505 K in the primary set, since for transient hot-wire measurements the correction for the finite outer boundary containing the gas becomes increasingly large due to the increasing thermal diffusivity of the gas as the pressure of the gas decreases. This correction becomes even more significant as the temperature increases and for outer boundaries less than 1 cm diameter, and is why we do not include in the primary data the low-density (<50 kg m⁻³) measurements made above 505 K. Steady-state hot-wire measurements of the dilute gas require much smaller corrections and have lower uncertainty than such transient hot-wire measurements with relatively large corrections for the finite outer boundary, and all steady-state low-density measurements made with double wires were included in the primary set, and single-wire steady-state measurements above

655 K. We also excluded from the primary data several points in the liquid phase where the equation of state calculated densities in the wrong phase for the given experimental temperature and pressure.

Finally, to extend the range of the measurements to high pressures, we added to the primary data 11 points from Tarzimanov and Arslanov³¹ that are in the liquid phase, and also 15 high-temperature (>550 K) high-pressure (>98 MPa) supercritical points. These measurements reported in Table 1 of Ref. 31 were made with a coaxial cylinder apparatus, and those in Table 2 of Ref. 31 are from a steady-state hot-wire apparatus; we have assigned an uncertainty of 3% to both sets.

Figure 1 shows the temperature and pressure range of the primary measurements outlined in Table 1 considered for use as primary data. The critical point, solid–liquid, solid–vapor, and vapor–liquid lines are also indicated. With the inclusion of the recent data of Perkins,⁷ there is now good coverage of the liquid phase up to 70 MPa. Temperatures for all data were converted to the ITS-90 temperature scale.¹¹³ The development of the correlation requires densities; Span and Wagner¹¹⁴ in 1996 reviewed the thermodynamic properties of carbon dioxide and developed an accurate, wide-ranging equation of state valid for the fluid region from the triple point to 1100 K at pressures up to 800 MPa. The estimated uncertainty in density ranges from 0.03% to 0.05% in the density at pressures up to 30 MPa and temperatures to 523 K. Special attention was given to the description of the critical region and the extrapolation behavior of the equation. We also adopt the values for the critical point and triple point from this equation of state; the critical temperature, T_c , and the critical density, ρ_c , were taken to be equal to 304.1282 K and 467.6 kg m⁻³, respectively, and the triple-point temperature is 216.592 K.¹¹⁴ We also adopt the correlation of Span and Wagner¹¹⁴ for the isobaric ideal-gas heat capacity, which is used in the theoretical model for the critical enhancement.

3.1. The dilute-gas limit

To develop the zero-density correlation, we follow the procedure used in the development of a standard reference formulation for the thermal conductivity of water,¹⁸ which

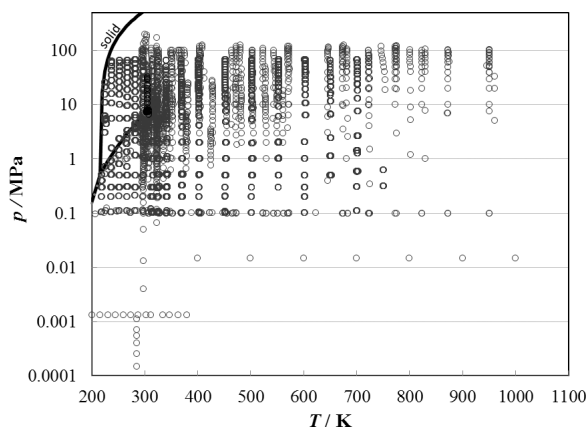


FIG. 1. Temperature and pressure ranges of the primary experimental thermal-conductivity data for carbon dioxide.

uses the concept of key comparison reference values¹¹⁵ to consider the uncertainties from different data sources. We first incorporated data sources^{25,26,28,29,33,40,42–44,89} used in the 1990 Vesovic correlation,⁵ with the uncertainty estimates as given in Table 1. As mentioned above, we retained only data at densities less than 50 kg m⁻³. To those points, we added the zero-density point of Imaishi *et al.*²⁷ obtained by analysis of an isotherm at 301 K at a range of densities in a transient hot-wire instrument, and three zero-density points presented in Snel *et al.*³⁰ that resulted from their analysis of a range of densities for three isotherms obtained in a hot-wire apparatus. One additional publication by Keyes⁴¹ was included, considering only points at densities under 50 kg m⁻³. We also considered all points at densities below our cutoff from the work of Haarman,³⁴ LeNeindre *et al.*,^{35,37,38} Li *et al.*,²⁴ Michels *et al.*,³⁹ and Bakulin *et al.*³² In addition, for Bakulin *et al.*,³² we considered only points at or below 1000 K. Finally, we included all double-wire measurements from the recent work of Perkins⁷ that were below the cutoff density except the transient data from Perkins⁷ for temperatures above 505 K as discussed earlier.

All low-density, primary data points were then arranged into bins encompassing a range of 8 K or less, with at least four data points in each bin. The average bin size was less than 3 K. Points that were already at zero density^{25–27,29,30} were not put into bins and were treated as separate isotherms. It was not possible to bin all points, since some exceeded the 8 K limit or failed to have at least four points. For example, it was not possible to include in a bin the data point of Franck at 197 K, so this point was not included in the primary data. This resulted in a total of 1328 points from 22 sources, obtained with a variety of experimental techniques and with a range of uncertainties.

The nominal temperature of an isotherm “bin” was computed as the average temperature of all points in a bin. The thermal conductivity of each point was then corrected to the nominal temperature, T_{nom} , by the following equation:

$$\lambda_{\text{corr}}(T_{\text{nom}}, \rho) = \lambda_{\text{exp}}(T_{\text{exp}}, \rho) + [\lambda(T_{\text{nom}}, \rho) - \lambda(T_{\text{exp}}, \rho)]_{\text{calc}}, \quad (2)$$

where the calculated values were obtained from the Vesovic *et al.*⁵ thermal-conductivity formulation.

Weighted linear regression was then used to extrapolate the nominal isotherms in order to obtain the value at zero density, λ_0 . The difference between the zero-density thermal conductivity and the value at a density of 50 kg m⁻³ is small enough that a linear expression can be used to extrapolate to zero density but needs to be taken into account; for example, at 500 K, the difference is about 5%. Points were weighted with a factor equal to the inverse of the square of the estimated relative uncertainty. 95% confidence intervals were constructed from the regression statistics. Isotherms with large inconsistencies in the underlying data were rejected from further consideration. The resulting set of zero-density data contained 47 points from 219 to 751 K.

In order to supplement the experimental data set at very low and at high temperatures where data are unavailable or sparse, we incorporated selected theoretical data points from the recent work of Hellmann.⁸ The theoretical calculations were made with a new four-dimensional rigid-rotor potential energy

surface, and the classical-trajectory method. We first adjusted the theoretical values by increasing their magnitude by a factor of 1.011 and ascribed to the theoretical values an uncertainty as recommended by Hellmann,⁸ namely, 1% for points between 300 and 700 K, increasing to 2% at 150 and 2000 K. The adjustment of 1.011 was recommended by Hellmann based on comparisons with the best available experimental data and accounts for uncertainties in the intermolecular potential. We included 8 points from 150 to 215 K, and 14 points from 760 to 2000 K, so that the final set of zero-density values range from 150 to 2000 K.

The zero-density values were fit using the orthogonal distance regression package ODRPACK (Ref. 116) to the same form of equation used in the water formulation¹⁸ for the thermal conductivity in the limit of zero density,

$$\lambda_0(T_r) = \frac{\sqrt{T_r}}{\sum_{k=0}^J \frac{L_k}{T_r^k}}, \quad (3)$$

where $T_r = T/T_c$ is a reduced temperature, and λ_0 is in $\text{mW m}^{-1} \text{K}^{-1}$. We used the critical temperature from the Span and Wagner equation of state,¹¹⁴ $T_c = 304.1282 \text{ K}$.

The final set of λ_0 values contained 69 data points from 150 to 2000 K and is shown in Fig. 2. The coefficients obtained from the regression are given in Table 3; we found a total of four terms was necessary. The initial weights were equal to the inverse of the square of the estimated uncertainty.

Figure 3 displays the percent deviation $(100(\lambda_{0,\text{exp}} - \lambda_{0,\text{cal}})/\lambda_{0,\text{cal}})$ between the λ_0 data and Eq. (3). Also shown are deviations with respect to the correlations of Vesovic *et al.*⁵ and Scalabrin *et al.*,⁶ and also with the theoretical calculations of Hellmann.⁸ The values of Hellmann have been scaled upward by a factor of 1.011 as mentioned earlier. The correlations of Vesovic *et al.*⁵ and Scalabrin *et al.*⁶ were valid only over the range 200–1000 K, and it is obvious that at low temperatures both do not extrapolate well. At high temperatures, the Vesovic *et al.*⁵ correlation extrapolates much better than Scalabrin *et al.*⁶ since Vesovic included theoretical considerations in the high-temperature behavior. The present work uses the theoretical calculations

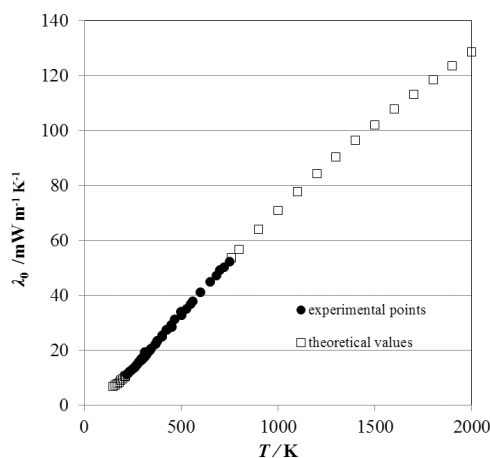


FIG. 2. Dataset for λ_0 used in the regression.

TABLE 2. Primary data considered for dilute-gas analysis

First author	No. of data	Uncertainty (%)	T range (K)	Density (kg m^{-3})
Perkins ⁷	1129	2–3	218–751	0.8–47.8
Li ²⁴	14	1.6	324	3–38
Millat ²⁵	4	1	308–426	0
Johns ²⁶	3	1	380–470	0
Imaishi ²⁷	1	0.5	301	0
Scott ²⁸	19	1	301–349	5–48
Clifford ²⁹	1	0.5	301	0
Snel ³⁰	3	1	293–323	0
Bakulin ³²	7	5	400–1000	0.1–0.2
Bakulin ³³	28	5	225–316	2–49
Haarman ³⁴	8	1	328–468	1.1–1.6
Le Neindre ^{35,36}	78	2–3	296–961	0.7–50
Le Neindre ³⁷	37	2–3	298–951	0.6–1.8
Le Neindre ³⁸	7	2–3	296–309	1.7–46
Michels ³⁹	20	1	298–348	1.6–49
Keyes ⁴⁰	2	5	207–273	2.0–2.5
Keyes ⁴¹	6	5	273–423	1.3–38
Lenoir ⁴²	5	2	314–340	1.7–40
Keyes ⁹³	5	5	223–473	23–48
Johnston ⁴³	14	1–5	186–380	0.02–0.04
Dickins ⁴⁴	6	1	285	0.03–0.2

of Hellmann⁸ to guide both the low- ($150 < T/\text{K} < 215$) and high-temperature ($760 < T/\text{K} < 2000$) behavior of the correlation, outside of the range of the best experimental data. Equation (3) may be extrapolated safely to 2000 K, the limit of the theoretical data included in the fit, although it does not take into account partial dissociation of CO_2 at high temperatures.¹¹⁷ The correlation of Vesovic *et al.*⁵ relied heavily on the works of Millat *et al.*²⁵ and Johns *et al.*,²⁶ particularly in the region 330–470 K, while this work considered additional data (primarily Perkins⁷) that tended to be lower than those of Millat *et al.*²⁵ and Johns *et al.*²⁶ and that are in closer agreement with Hellmann.⁸ Since there is considerable scatter in the experimental points, with many of the underlying data not in agreement within their stated uncertainties, we consider the comparisons with the scaled theoretical values of Hellmann⁸ to assess the uncertainty of the dilute-gas correlation. The theoretical values have an estimated uncertainty of 1% between 300 and 700 K, increasing to 2%

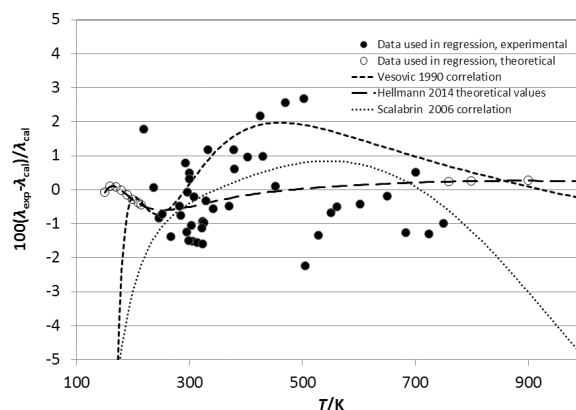


FIG. 3. Comparison of λ_0 correlations with the theoretical and experimental data.

TABLE 3. Coefficients in Eq. (3) for λ_0

k	L_k
0	$1.518\,743\,07 \times 10^{-2}$
1	$2.806\,740\,40 \times 10^{-2}$
2	$2.285\,641\,90 \times 10^{-2}$
3	$-7.416\,242\,10 \times 10^{-3}$

at both 150 and 2000 K, and we adopt those values for our uncertainty estimate for Eq. (3).

3.2. The residual thermal conductivity

The thermal conductivities of pure fluids exhibit an enhancement over a large range of densities and temperatures around the critical point and become infinite at the critical point. This behavior can be described by models that produce a smooth crossover from the singular behavior of the thermal conductivity asymptotically close to the critical point to the background values far away from the critical point.^{118–120} The density-dependent terms for thermal conductivity can be grouped according to Eq. (1) as $[\Delta\lambda(\rho, T) + \Delta\lambda_c(\rho, T)]$. To assess the critical enhancement either theoretically or empirically, we need to evaluate, in addition to the dilute-gas thermal conductivity, the residual thermal-conductivity contribution. The procedure adopted during this analysis used ODRPACK (Ref. 116) to fit the primary data to determine the coefficients of the residual thermal conductivity, Eq. (4), while maintaining the values of the dilute-gas thermal conductivity obtained by Eq. (3) and calculating the critical enhancement with the model discussed in Sec. 3.3.1. The density values employed were obtained by the equation of state of Span and Wagner.¹¹⁴ The residual thermal conductivity was represented with a polynomial in temperature and density,

$$\Delta\lambda(\rho, T) = \sum_{i=1}^6 (B_{1,i} + B_{2,i}(T/T_c))(\rho/\rho_c)^i. \quad (4)$$

During the regression process, it was found that the residual contribution as given by Eq. (4) does not require the temperature-dependent coefficients $B_{2,i}$ for representation of supercritical and vapor-phase data. This also was pointed out by Vesovic *et al.*⁵ However, we found that allowing for temperature dependence of the residual contribution improved the representation of the liquid-phase data at high pressures (especially above 70 MPa), and we have included temperature coefficients $B_{2,i}$ in our correlation. The coefficients $B_{1,i}$ and $B_{2,i}$ are shown in Table 4.

3.3. The critical enhancement

The thermal conductivity and viscosity of a pure fluid diverge at the critical point.^{121,122} The thermal diffusivity, $a = \lambda/\rho C_p$, approaches zero at the critical point since the isobaric specific heat, C_p , diverges more rapidly than the thermal conductivity.¹²² Data for thermal diffusivity can be converted to thermal-conductivity data when accurate values

TABLE 4. Coefficients of Eq. (4) for the residual thermal conductivity of carbon dioxide

i	$B_{1,i}$ (W m ⁻¹ K ⁻¹)	$B_{2,i}$ (W m ⁻¹ K ⁻¹)
1	$1.001\,28 \times 10^{-2}$	$4.308\,29 \times 10^{-3}$
2	$5.604\,88 \times 10^{-2}$	$-3.585\,63 \times 10^{-2}$
3	$-8.116\,20 \times 10^{-2}$	$6.714\,80 \times 10^{-2}$
4	$6.243\,37 \times 10^{-2}$	$-5.228\,55 \times 10^{-2}$
5	$-2.063\,36 \times 10^{-2}$	$1.745\,71 \times 10^{-2}$
6	$2.532\,48 \times 10^{-3}$	$-1.964\,14 \times 10^{-3}$

for the density and isobaric specific heat are available or can be calculated at the measurement conditions with an equation of state. Thermal-conductivity data obtained from thermal diffusivity data have additional uncertainty associated with the ρ and C_p values that must be considered. Thus, it was decided to base the correlation on direct determinations of the thermal conductivity.

Thermal diffusivity data from light scattering are available much closer to the critical point and have the advantage in the critical region of not requiring a macroscopic temperature gradient, with a corresponding density gradient that can drive convection during thermal conductivity measurements. It was further decided to validate the critical enhancement model with the thermal diffusivity data very close to the critical point where thermal-conductivity data are not available.

3.3.1. Simplified crossover model

The theoretically based crossover model proposed by Olchowy and Sengers^{118–120} is complex and requires solution of a quartic system of equations in terms of complex variables.

TABLE 5. Evaluation of the carbon dioxide thermal-conductivity correlation for the primary data^a

First author	Year of publication	No. of data	AAD (%)	BIAS (%)
Perkins ⁷	2016	4095	1.42	-0.63
Li ²⁴	1994	14	0.39	0.12
Millat ²⁵	1987	78	0.80	-0.70
Johns ²⁶	1986	46	0.40	-0.04
Imaishi ²⁷	1984	23	0.56	-0.27
Scott ²⁸	1983	47	1.23	-0.96
Clifford ²⁹	1979	20	0.49	-0.23
Snel ³⁰	1979	93	1.63	-1.63
Tarzimanov ³¹	1978	26	1.92	1.80
Bakulin ³²	1976	7	1.31	-1.05
Bakulin ³³	1975	28	1.33	0.08
Haarman ³⁴	1973	8	0.37	-0.35
Le Neindre ^{35,36}	1973	528	1.57	-0.28
LeNeindre ³⁷	1972	193	1.47	0.27
Le Neindre ³⁸	1968	27	2.14	0.64
Michels ^{39,a}	1962	162	2.79	-1.69
Keyes ⁴⁰	1955	2	0.98	-0.55
Keyes ⁴¹	1951	7	0.95	0.18
Lenoir ⁴²	1951	3	0.70	0.70
Johnston ⁴³	1946	14	0.82	-0.05
Dickins ⁴⁴	1934	6	0.81	-0.81
Entire data set		5427	1.5	-0.6

^aData within ± 1 K of the critical temperature excluded.

TABLE 6. Evaluation of the carbon dioxide thermal-conductivity correlation for all data sets

First author	Year of publication	No. of data	AAD (%)	BIAS (%)
Perkins ⁷	2016	4824	4.1	2.2
Tomida ⁴⁵	2010	19	1.3	−0.6
Patek ⁴⁶	2005	77	0.7	−0.4
Heinemann ⁴⁷	2000	3	4.7	4.7
Chen ⁴⁸	1999	66	38.6	35.7
Dohrn ⁴⁹	1999	7	4.3	4.3
Li ²⁴	1994	14	0.4	0.1
Millat ²⁵	1987	91	0.8	−0.4
Johns ²⁶	1986	47	0.5	−0.2
Imaishi ²⁷	1984	23	0.6	−0.3
Zheng ⁵⁰	1984	13	0.5	−0.2
Scott ²⁸	1983	92	2.1	0.6
Yorizane ⁵¹	1983	15	1.2	0.3
Clifford ²⁹	1979	22	0.5	−0.2
Snel ³⁰	1979	133	1.4	−1.4
Becker ⁵²	1978	217	7.7	−1.0
Tarzimanov ³¹	1978	94	2.8	2.5
Ulybin ⁵³	1977	14	2.0	0.6
Bakulin ³²	1976	10	2.7	−2.6
Bakulin ³³	1975	28	1.3	0.1
Chen ⁵⁴	1975	34	4.6	−4.6
Haarman ³⁴	1973	8	0.4	−0.4
LeNeindre ^{35,36}	1973	536	1.6	−0.2
Salmanov ⁵⁵	1973	19	3.3	3.3
Shashkov ⁵⁶	1973	9	1.4	−1.0
Dijkema ⁵⁷	1972	2	4.0	−4.0
LeNeindre ³⁷	1972	194	1.5	0.2
Gupta ⁵⁸	1970	11	5.2	−5.2
Maczek ⁵⁹	1970	1	1.9	−1.9
Murthy ⁶⁰	1970	3	1.3	0.9
Murthy ⁶¹	1970	53	33.3	29.4
Tarzimanov ⁶²	1970	52	50.3	49.1
Golubev ⁶³	1969	733	9.9	9.1
Rosenbaum ⁶⁴	1969	50	2.8	0.3
Barua ⁶⁵	1968	5	2.2	−2.1
LeNeindre ³⁸	1968	31	2.2	0.8
Shingarev ⁶⁶	1968	23	3.8	−0.8
van Dael ⁶⁷	1968	1	1.5	−1.5
Freud ⁶⁸	1967	42	6.0	1.6
Mukhopadhyay ⁶⁹	1967	7	1.7	−0.9
Mukhopadhyay ⁷⁰	1967	5	2.2	−2.1
Baker ⁷¹	1964	1	1.9	−1.9
Senftleben ⁷²	1964	8	2.3	0.9
Amirkhanov ⁷³	1963	20	22.6	−22.2
Michels ³⁹	1962	253	11.8	6.4
Cheung ⁷⁴	1962	2	1.1	−1.1
Guildner ⁷⁵	1962	39	10.3	8.0
Westenberg ⁷⁶	1962	3	1.5	−1.5
Geier ⁷⁷	1961	23	9.6	−8.9
Vines ⁷⁸	1960	4	1.2	0.5
Chaikin ⁷⁹	1958	5	5.4	−5.4
Guildner ⁸⁰	1958	22	15.6	13.5
Waelbroeck ⁸¹	1958	1	1.0	−1.0
Salceanu ⁸²	1956	1	6.2	−6.2
Keyes ⁴⁰	1955	2	1.0	−0.6
Kulakov ⁸³	1955	2	64.9	−64.9
Rothman ⁸⁴	1955	2	4.9	−4.9
Filippov ⁸⁵	1954	6	13.1	4.3
Thomas ⁸⁶	1954	4	1.5	−1.5
Davidson ⁸⁷	1953	1	3.8	−3.8
Rothman ⁸⁸	1953	25	3.6	−2.2
Franck ⁸⁹	1951	7	4.8	−4.8
Keyes ⁴¹	1951	9	1.6	1.0
Lenoir ⁴²	1951	32	4.4	4.4

TABLE 6. Evaluation of the carbon dioxide thermal-conductivity correlation for all data sets—Continued

First author	Year of publication	No. of data	AAD (%)	BIAS (%)
Kannuiliuk ⁹⁰	1950	9	2.7	−2.7
Stolyarov ⁹¹	1950	17	8.0	3.1
Borovik ⁹²	1949	18	7.0	−6.8
Keyes ⁹³	1949	8	4.6	−4.5
Stops ⁹⁴	1949	1	1.3	1.3
Timrot ⁹⁵	1949	160	11.8	−0.7
Kannuiliuk ⁹⁶	1947	15	1.6	1.5
Johnston ⁴³	1946	14	0.8	0.0
Vargaftik ⁹⁷	1946	13	2.7	−2.7
Eucken ⁹⁸	1940	6	5.3	−4.8
Koch ⁹⁹	1940	54	5.2	−4.8
Sherratt ¹⁰⁰	1939	10	2.0	1.8
Archer ¹⁰¹	1935	11	6.4	−6.4
Dickins ⁴⁴	1934	6	0.8	−0.8
Kannuiliuk ¹⁰²	1934	1	2.3	−2.3
Kardos ¹⁰³	1934	6	150.2	150.2
Sellschopp ¹⁰⁴	1934	50	7.7	0.6
Trautz ¹⁰⁵	1933	19	29.2	22.6
Kornfeld ¹⁰⁶	1931	1	2.6	2.6
Gregory ¹⁰⁷	1927	6	0.6	0.2
Weber ¹⁰⁸	1927	1	2.6	−2.6
Weber ¹⁰⁹	1917	1	3.7	−3.7
Schleiermacher ¹¹⁰	1888	1	2.0	2.0
Graetz ¹¹¹	1881	1	11.1	−11.1
Winkelmann ¹¹²	1880	1	13.5	−13.5

A simplified crossover model has also been proposed by Olchoway and Sengers.¹²³ The critical enhancement of the thermal conductivity from this simplified model is given by

$$\Delta\lambda_c = \frac{\rho C_p R_D k_B T}{6\pi\eta\xi} (\bar{\Omega} - \bar{\Omega}_0), \quad (5)$$

with

$$\bar{\Omega} = \frac{2}{\pi} \left[\left(\frac{C_p - C_v}{C_p} \right) \arctan(\bar{q}_D \xi) + \frac{C_v}{C_p} \bar{q}_D \xi \right] \quad (6)$$

and

$$\bar{\Omega}_0 = \frac{2}{\pi} \left[1 - \exp \left(- \frac{1}{(\bar{q}_D \xi)^{-1} + (\bar{q}_D \xi \rho_c / \rho)^2 / 3} \right) \right]. \quad (7)$$

In Eqs. (5)–(7), k_B is Boltzmann's constant, η is the viscosity, and C_p and C_v are the isobaric and isochoric specific heat. All thermodynamic properties were obtained from the equation of state of Span and Wagner.¹¹⁴ To estimate the viscosity, one can use either the correlation of Fenghour *et al.*¹²⁴ or the new correlation of Laesecke and Muzny.¹²⁵ Both are implemented in the REFPROP (Ref. 126) program; the results reported here use the new formulation.¹²⁵ The correlation length ξ is given by

$$\xi = \xi_0 \left(\frac{p_c \rho}{\Gamma \rho_c^2} \right)^{\nu/\gamma} \left[\left. \frac{\partial \rho(T, \rho)}{\partial p} \right|_T - \left(\frac{T_{\text{ref}}}{T} \right) \left. \frac{\partial \rho(T_{\text{ref}}, \rho)}{\partial p} \right|_T \right]^{\nu/\gamma}. \quad (8)$$

This crossover model requires the universal constants¹²¹ $R_D = 1.02$, $\nu = 0.63$, and $\gamma = 1.239$, and system-dependent amplitudes Γ and ξ_0 . For this work, as was done previously by Vesovic *et al.*,⁵ we adopted the values $\Gamma = 0.052$ and ξ_0

$= 1.50 \times 10^{-10}$ m, determined specifically for carbon dioxide,¹²⁷ instead of using the general method presented by Perkins *et al.*¹²¹ The reference temperature T_{ref} , far above the critical temperature where the critical enhancement is negligible, was calculated by $T_{\text{ref}} = (3/2)T_c$,¹²¹ which for carbon dioxide is 456.19 K. The only critical-region parameter that needs to be determined is \bar{q}_D . We used the effective cutoff wavelength \bar{q}_D^{-1} found in the work of Vesovic *et al.*,⁵ 4.0×10^{-10} m. The equation of state of Span and Wagner¹¹⁴ displays some unphysical behavior at temperatures very close to the critical point that affects the heat capacity and the derivative of density with respect to pressure, so all data within 1 K of the critical point were excluded from the regression, and the set of $B_{1,i}$ coefficients was obtained. The scaled equation of state of Albright *et al.*¹²⁷ was then used to validate this value of \bar{q}_D and the background coefficients of Eq. (4), with both thermal conductivity and thermal diffusivity data within 1 K of critical as discussed in Sec. 3.3.2.

Table 5 summarizes comparisons of the primary data with the correlation. We have defined the percent deviation as $\text{PCTDEV} = 100(\lambda_{\text{exp}} - \lambda_{\text{cal}})/\lambda_{\text{cal}}$, where λ_{exp} is the experimental value of the thermal conductivity and λ_{cal} is the value calculated from the correlation. Thus, the average absolute percent deviation (AAD) is found with the expression $\text{AAD} = (\sum |\text{PCTDEV}|)/n$, where the summation is over all n points, and the bias percent is found with the expression $\text{BIAS} = (\sum \text{PCTDEV})/n$. Table 6 summarizes the deviations over all data sets.

Figure 4 shows the percentage deviation of the primary data for the subcritical vapor region (densities from 0.02 to 341.81 kg m⁻³, pressures from 0.0001 to 7.2 MPa) as a function of temperature, while Fig. 5 shows the deviations as a function of pressure. The data sets with the lowest uncertainties cover only the region very close to 300 K (298 to 304 K) and are Imaishi *et al.*,²⁷ Clifford *et al.*,²⁹ and Snel *et al.*³⁰ There is a systematic offset for Snel *et al.*³⁰ due to the dilute-gas correlation, but all three of these data sets are represented to within 1%. The measurements of Perkins⁷ cover the broader range of temperatures from 218 to 299 K, at pressures from

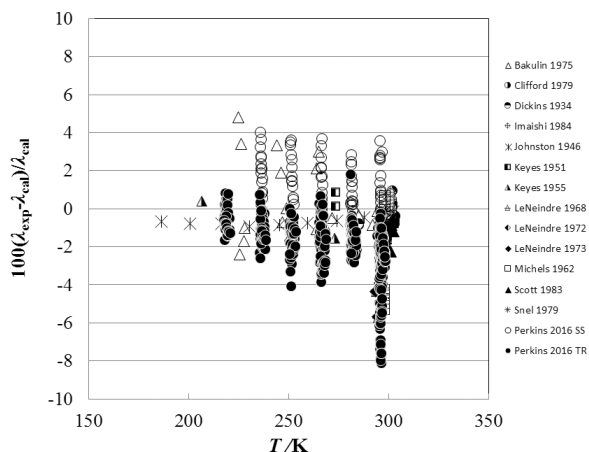


FIG. 4. Percentage deviations of primary experimental data of carbon dioxide from the values calculated by the present model as a function of temperature, for the vapor region.

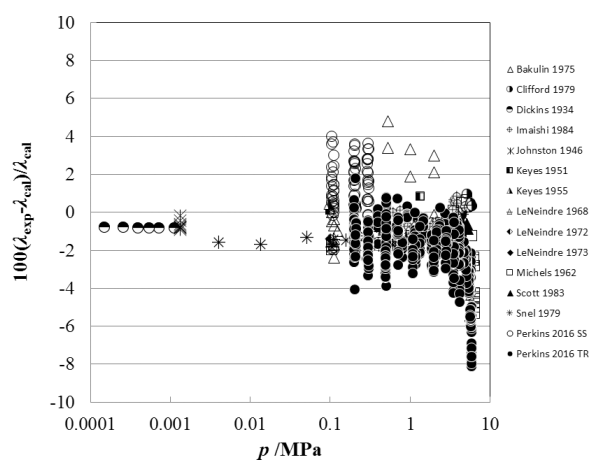


FIG. 5. Percentage deviations of primary experimental data of carbon dioxide from the values calculated by the present model as a function of pressure, for the vapor region.

0.1 to 5.5 MPa. The steady-state measurements of Perkins with the low-temperature apparatus are systematically higher than the transient results, but still generally within the estimated uncertainty of $\pm 3\%$. This is likely due to increased uncertainty in the temperature rise measurement; the low-temperature instrument only has three leads within the pressure vessel so the potential across each hot wire is measured with wires that also carry the measurement current. As the critical temperature and pressure are approached, the Michels *et al.*³⁹ data show larger deviations; data within 1 K of critical have been excluded from the plot.

Figure 6 shows the percentage deviation of the primary data for the supercritical region at temperatures up to 500 K (densities from 0.02 to 341.81 kg m⁻³, pressures from 0.0001 to 7.2 MPa) as a function of temperature, while Fig. 7 shows the deviations as a function of pressure. In this region, the measurements of Haarman³⁴ and Snel *et al.*³⁰ are represented to within 1%, although there is a systematic offset for Snel *et al.*³⁰ due to the dilute-gas correlation. The steady-state hot-wire measurements of Perkins range up to 70 MPa and are represented to within their experimental uncertainty of 2%.

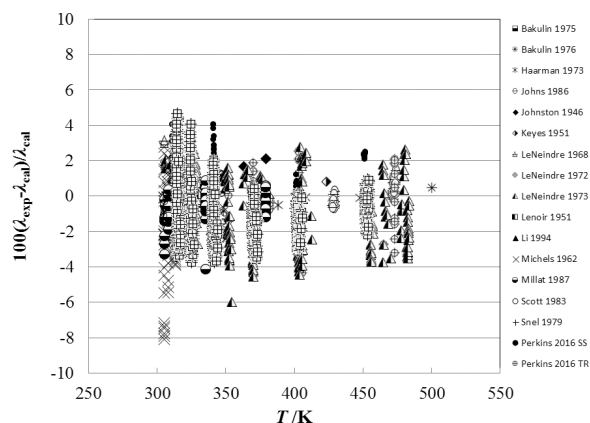


FIG. 6. Percentage deviations of primary experimental data of carbon dioxide from the values calculated by the present model as a function of temperature, for the supercritical region at temperatures up to 500 K.

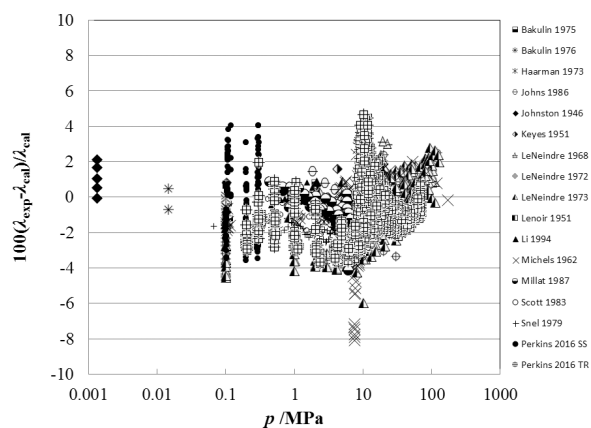


FIG. 7. Percentage deviations of primary experimental data of carbon dioxide from the values calculated by the present model as a function of pressure, for the supercritical region at temperatures to 500 K.

The other measurements (transient method) of Perkins in the temperature region from the critical temperature to 500 K have a slightly higher uncertainty, 3%, and are also represented to within 2%.

Figure 8 shows the percentage deviation of the primary data for temperatures above 500 K as a function of temperature, while Fig. 9 shows the deviations as a function of pressure. The measurements of Perkins,⁷ extending to 70 MPa, are represented to within their estimated uncertainty, 3%. The measurements of LeNeindre *et al.*,^{35,37} Bakulin *et al.*,³² and Tarzimanov and Arslanov³¹ also fall within 3%.

Figure 10 shows the percentage deviations of the primary data in the liquid phase as a function of temperature, and Fig. 11 shows the same as a function of pressure, excluding data within 1 K of critical. The measurements of Perkins in this region have an estimated uncertainty of 0.5%, and the correlation represents the data to within 1%. Comparisons with the data of Tarzimanov and Arslanov³¹ show deviations lower than 3% at pressures to 196 MPa. As the critical region is approached, the deviations become larger. One of the motivations for this work was to incorporate the new liquid-phase measurements of Perkins⁷ to allow improvement in the representation of

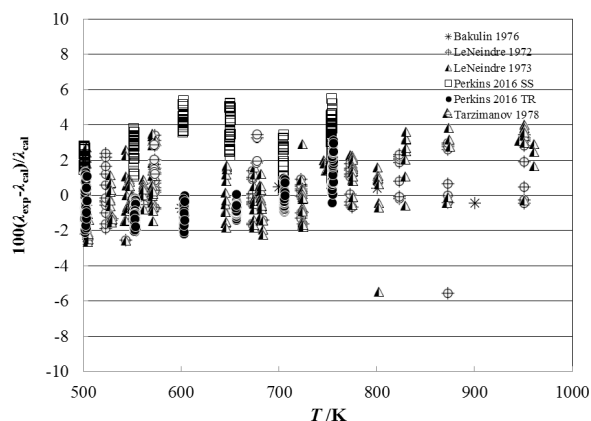


FIG. 8. Percentage deviations of primary experimental data of carbon dioxide from the values calculated by the present model as a function of temperature, for the supercritical region at temperatures above 500 K.

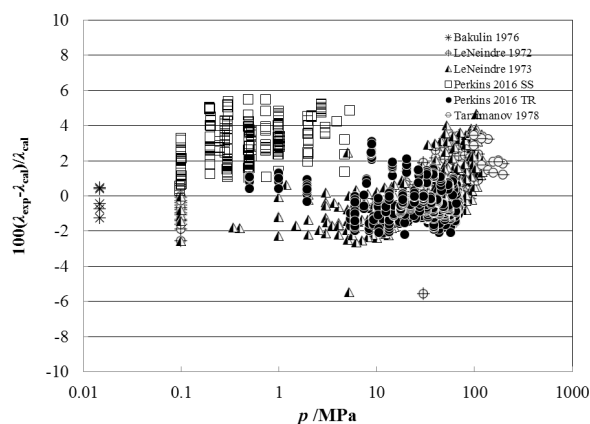


FIG. 9. Percentage deviations of primary experimental data of carbon dioxide from the values calculated by the present model as a function of pressure, for the supercritical region at temperatures above 500 K.

the liquid phase. Figures 12 and 13 show the percentage deviations of the primary data in the liquid phase as a function of temperature for the previous correlations of Vesovic *et al.*⁵ (Fig. 12) and Scalabrin *et al.*⁶ (Fig. 13). Upon comparing these two figures with Fig. 10, the improvement in the representation of the liquid phase is shown.

3.3.2. Thermal diffusivity validation

The thermal-conductivity model described above is based entirely on reliable thermal-conductivity data that were measured at temperatures where the equation of state of Span and Wagner¹¹⁴ is accurate. The scaled equation of state of Albright *et al.*¹²⁷ provides better values for the thermodynamic properties in the temperature region ($303.1282 \leq T/K \leq 305.1282$) with densities ($350 \leq \rho/\text{kg m}^{-3} \leq 530$). The Albright *et al.*¹²⁷ equation of state was also used in the 1990 correlation of Vesovic *et al.*⁵ where it was required over a larger temperature region ($301.15 \leq T/K \leq 323$) and density region ($290 \leq \rho/\text{kg m}^{-3} \leq 595$). The Albright *et al.*¹²⁷ scaled equation of state was based on the IPTS-68 temperature scale, so we have used it here with the ITS-90 values for the critical

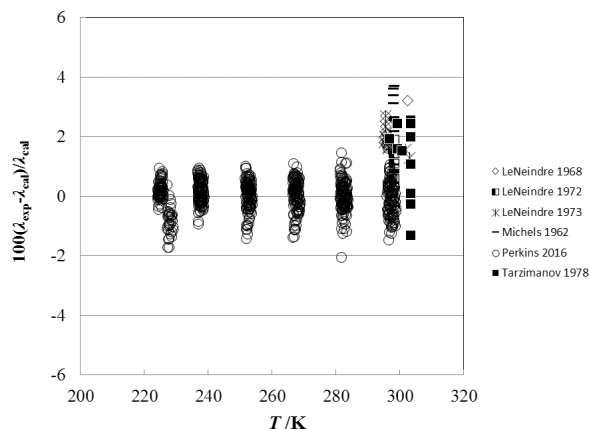


FIG. 10. Percentage deviations of primary experimental data of carbon dioxide from the values calculated by the present model as a function of temperature, for the liquid phase.

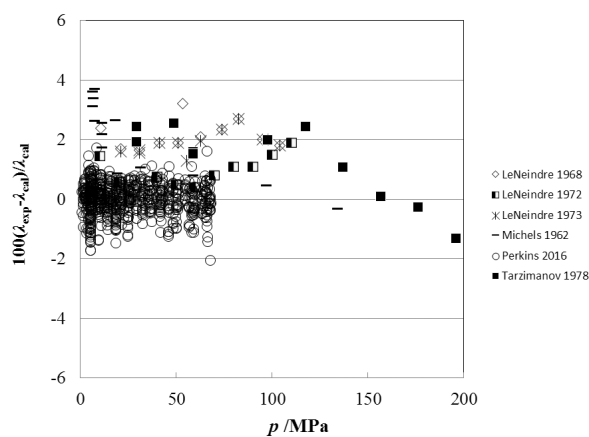


FIG. 11. Percentage deviations of primary experimental data of carbon dioxide from the values calculated by the present model as a function of pressure, for the liquid phase.

point of CO₂ from the equation of state of Span and Wagner¹¹⁴ to effectively convert it to the ITS-90 temperature scale.

The thermal diffusivity of CO₂ was measured with transient interferometry of the fluid below a horizontal heated surface near its critical point by Becker and Grigull.⁵² These measurements were reported along one liquid isotherm at 298.147 K and three supercritical isotherms at 304.362, 305.228, and 307.958 K (converted to ITS-90) and are shown in Fig. 14 along with curves calculated with the correlation of this work and thermodynamic properties from the Albright *et al.*¹²⁷ scaled equation of state. Only the isotherm at 304.362 K requires the scaled equation of state,¹²⁷ but it is valid at all of these temperatures. Unphysical behavior is visible in the values calculated with the Span and Wagner¹¹⁴ equation of state (dashed line) at 304.362 K, seen more easily in the inset in Fig. 14.

The thermal diffusivity of CO₂ was also determined from light-scattering measurements of the width of the Rayleigh line.^{128–131} Here, we will focus on the measurements of Swinney and Henry¹²⁸ where tabular results were given. The other light-scattering data are consistent with these results. Swinney and Henry¹²⁸ provide the Rayleigh line width, Γ ,

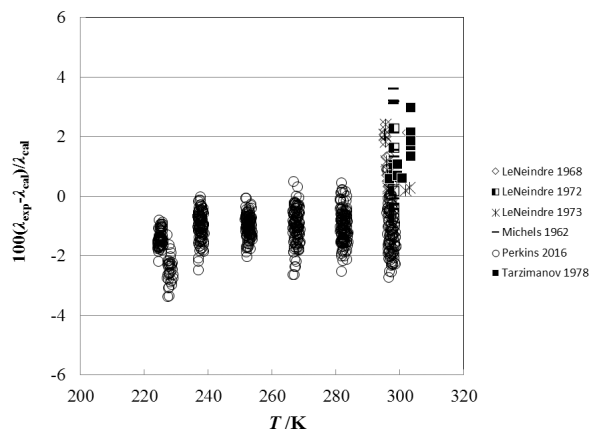


FIG. 12. Percentage deviations of primary experimental data of carbon dioxide from the values calculated by the Vesovic *et al.*⁵ model as a function of temperature, for the liquid phase.

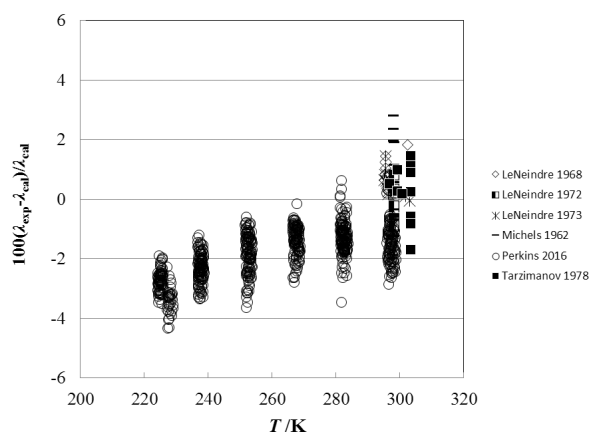


FIG. 13. Percentage deviations of primary experimental data of carbon dioxide from the values calculated by the Scalabrin *et al.*⁶ model as a function of temperature, for the liquid phase.

and the magnitude of the scattering vector, q , as a function of $(T - T_c)$ along the critical isochore. The thermal diffusivity can be obtained from these values with the expression

$$a = \frac{\Gamma}{\left(\frac{3}{4\xi^2}\right) \left[1 + q^2\xi^2 + \left(q^3\xi^3 - \frac{1}{q\xi}\right) \arctan(q\xi)\right]}, \quad (9)$$

as shown by Kawasaki¹³² and applied by Henry *et al.*¹³³ Equation (9) requires values for the correlation length, ξ , which were calculated with the Albright *et al.*¹²⁷ scaled equation of state. Alternatively, along the critical isochore, $\xi = \xi_0[(T - T_c)/T_c]^{-\nu}$ with ξ_0 and ν given in Sec. 3.3.1. Values of the thermal diffusivity, a , calculated from the light-scattering data of Swinney and Henry¹²⁸ with Eq. (9) are shown in Fig. 15. The correlation for thermal conductivity

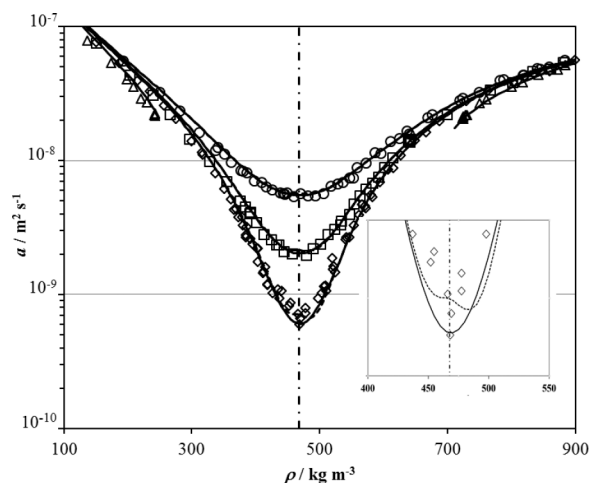


FIG. 14. Thermal diffusivity of CO₂ measured with interferometry of the fluid sample below a transient heated plate by Becker and Grigull⁵² along isotherms near the critical point. The isotherms are designated by symbols: Δ , 298.147 K; \diamond , 304.362 K; \square , 305.228 K; \circ , 307.958 K. The dashed lines show the calculated thermal diffusivity with the present correlation with the Span and Wagner¹¹⁴ equation of state and the solid lines show the calculated thermal diffusivity with the present correlation with the Albright *et al.*¹²⁷ scaled equation of state. The critical density is shown with the dotted-dashed line.

developed here is consistent with the thermal diffusivity from light scattering to within $(T - T_c) = 0.006$ K when used with the Albright *et al.*¹²⁷ scaled equation of state. The equation of state of Span and Wagner¹¹⁴ exhibits increasing errors near the critical point as indicated by the dashed line.

Finally, the thermal diffusivity data of Becker and Grigull⁵² are converted to thermal-conductivity values for comparison with the direct thermal-conductivity measurements of Michels *et al.*³⁹ made with a steady-state parallel plate apparatus in the critical region. The thermal-conductivity isotherms are shown in Fig. 16. Good agreement is found between the thermal-conductivity data of Michels *et al.*³⁹ and the

thermal conductivity obtained from the thermal diffusivity data of Becker and Grigull.⁵² As in Fig. 14, the values calculated for thermal conductivity at 304.36 K exhibit unphysical behavior for the Span and Wagner¹¹⁴ equation of state (dashed line).

3.3.3. Empirical critical enhancement

For engineering applications at state points that are more than 10 K from the critical point, the critical enhancement (in $\text{mW m}^{-1} \text{K}^{-1}$) can be represented to within about 5% by the following empirical expression:

$$\Delta\lambda_c(\rho, T) = \frac{-17.47 - 44.88\Delta T_c}{0.8563 - \exp[8.865\Delta T_c + 4.16\Delta\rho_c^2 + 2.302\Delta T_c\Delta\rho_c - \Delta\rho_c^3] - 0.4503\Delta\rho_c - 7.197\Delta T_c}, \quad (10)$$

where $\Delta T_c = (T/T_c) - 1$ and $\Delta\rho_c = (\rho/\rho_c) - 1$. This equation does not require accurate information on the compressibility, specific heat, and viscosity of carbon dioxide in the critical region, as does the theory of Olchowy and Sengers.¹²³ However, it has no theoretical basis at all and does not go to the theoretical limit at the critical point. It was obtained by using a symbolic regression program¹³⁴ to fit the primary data with the background [Eqs. (3) and (4)] coefficients fixed. This is an unusual function with poles, but they occur well within the two-phase region and do not affect the calculation of the enhancement. Simpler empirical enhancement terms such as those used in previous publications^{11–17} were investigated, but Eq. (10) gave superior results. Figure 17 shows the percentage deviations between all primary data (excluding values within 1 K of critical) and the values calculated by Eqs. (1) and (3)–(8), as a function of the temperature, while Fig. 18 shows

the same calculated instead with Eqs. (1), (3), (4), and (10). By comparing Figs. 17 and 18, it can be seen that employing Eq. (10) is an adequate empirical representation of the thermal conductivity surface excluding the region within 10 K of the critical temperature.

4. Uncertainty Assessments

4.1. Uncertainty outside of the critical region

Figure 19 shows the estimated uncertainty of the correlation at a 95% confidence level. As indicated in the figure, for the vapor region below critical at pressures from 0.1 MPa to slightly below the critical pressure (~ 7 MPa), the estimated

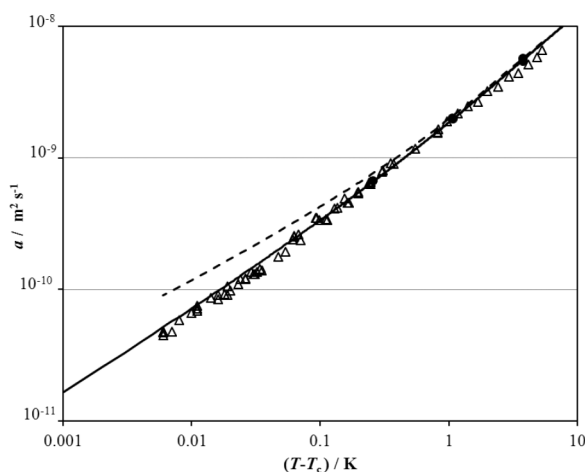


FIG. 15. Thermal diffusivity of CO_2 along the critical isochore close to the critical temperature from the Rayleigh scattering line width from Swinney and Henry¹²⁸ (Δ) and the transient interferometry measurements of Becker and Grigull⁵² (\bullet). Solid curve is from the correlation for thermal conductivity described here with thermodynamic properties from the Albright *et al.*¹²⁷ equation of state. Dashed curve is based on properties from the Span and Wagner¹¹⁴ equation of state.

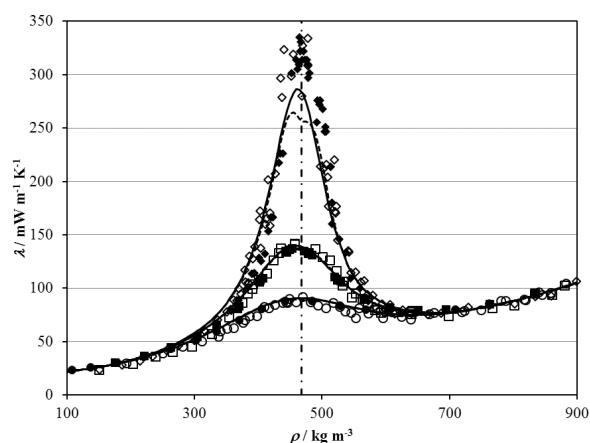


FIG. 16. Thermal conductivity along isotherms near the critical point measured directly by Michels *et al.*³⁹ and calculated from the thermal diffusivity data of Becker and Grigull⁵² with ρ and C_p from the Albright *et al.* equation of state.¹²⁷ Michels *et al.*³⁹ thermal-conductivity isotherms are designated by symbols: \blacklozenge , 304.357 K; \blacksquare , 305.271 K; \bullet , 307.848 K. Becker and Grigull⁵² isotherms are designated by symbols: \diamond , 304.362 K; \square , 305.228 K; \circ , 307.958 K. The dashed lines show the calculated thermal conductivity with the present correlation with the Span and Wagner¹¹⁴ equation of state and the solid lines show the calculated thermal conductivity with the present correlation with the Albright *et al.*¹²⁷ scaled equation of state. The critical density is shown with the dotted-dashed line.

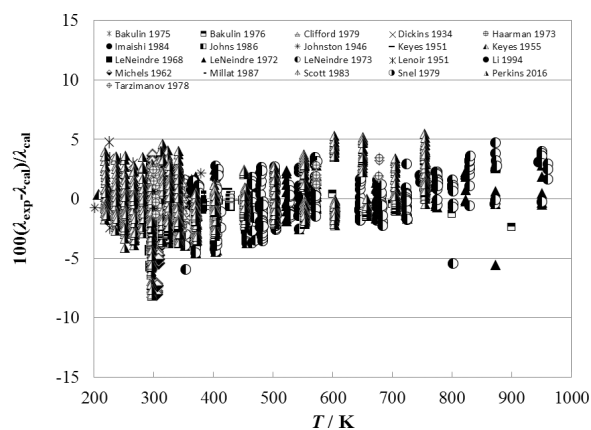


FIG. 17. Percentage deviations of all primary experimental data of carbon dioxide from the values calculated by the full model Eqs. (1) and (3)–(8) as a function of temperature.

uncertainty is 3%. This is an improvement over the previous correlation of Vesovic *et al.*,⁵ which had an uncertainty of 5% in this region. The improvement is due to the availability of the new data of Perkins.⁷ The liquid region, at temperatures from 224 to 299 K at pressures to 70 MPa, is another region where the availability of new data has enabled improvements in the surface. Previously, the correlation of Vesovic *et al.*⁵ had an uncertainty estimate of 5% in this region; the present correlation has 1% uncertainty. Similarly, the availability of the new data of Perkins at temperatures to 750 K and pressures to 70 MPa made it possible to lower the uncertainty to 3% for this supercritical region. At very low pressures below 0.1 MPa, the correlation has an estimated uncertainty of 1% between 300 and 700 K, increasing to 2% at both 150 and 2000 K. Additional future measurements in the remaining areas of the pressure–temperature space at high temperatures and high pressures are desirable to allow further reductions in uncertainty for the thermal conductivity surface.

4.2. Uncertainty in the critical region

Figures 14–16 show that the critical enhancement calculated with ξ and C_p from the Albright *et al.*¹²⁷ scaled equation

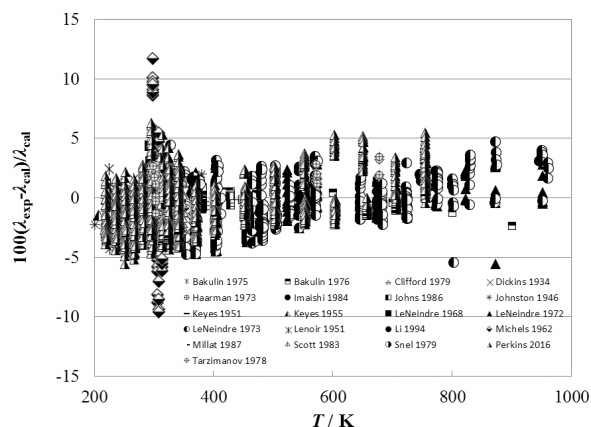


FIG. 18. Percentage deviations of all primary experimental data of carbon dioxide from the values calculated by the empirical critical enhancement model Eqs. (1), (3), (4), and (10) as a function of temperature.

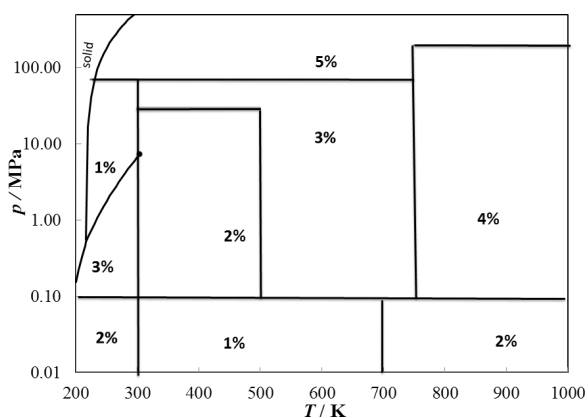


FIG. 19. Estimated uncertainty for the correlation excluding the critical region.

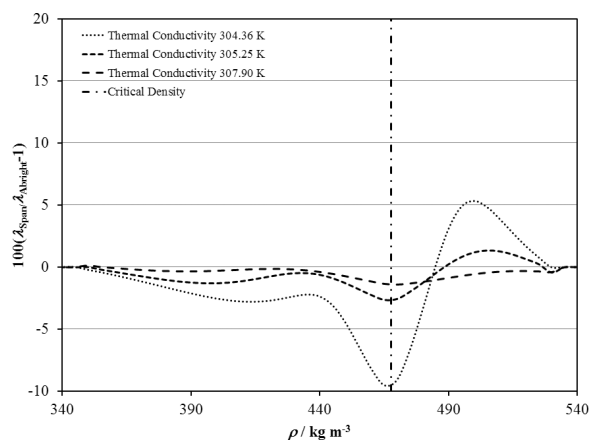


FIG. 20. Deviations in λ for the present correlation with thermodynamic properties calculated with the equation of state of Span and Wagner¹¹⁴ relative to the Albright *et al.*¹²⁷ scaled equation of state in the critical region.

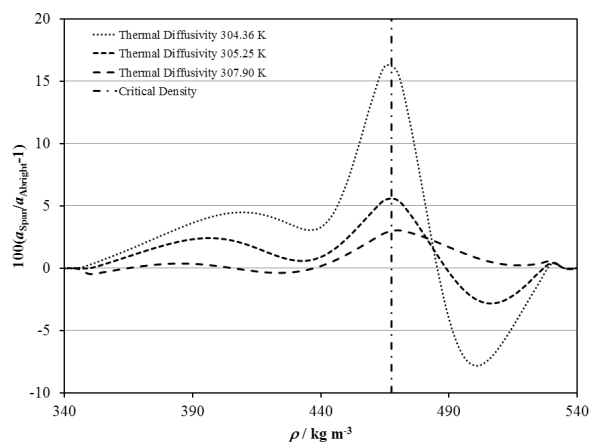


FIG. 21. Deviations in a for the present correlation with thermodynamic properties calculated with the equation of state of Span and Wagner¹¹⁴ relative to the Albright *et al.*¹²⁷ scaled equation of state in the critical region.

of state better represents the data in the critical region due to the limitations of the Span and Wagner¹¹⁴ equation of state. Figures 20 and 21 show differences between λ and a , respectively, calculated with each of these equations of state along the isotherms near 304.36, 305.25, and 307.90 K where reliable thermal conductivity and thermal diffusivity data are

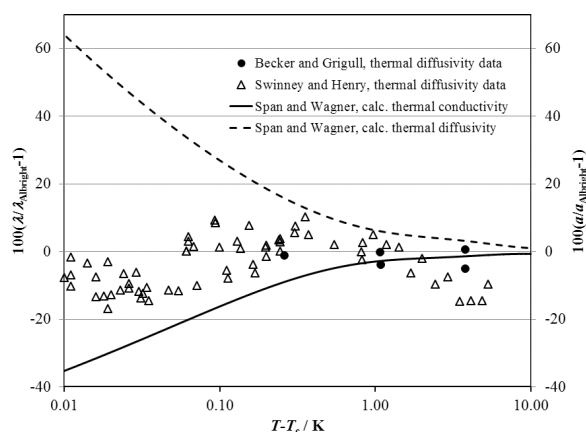


FIG. 22. Deviations in λ and α for the present correlation with thermodynamic properties calculated with the equation of state of Span and Wagner¹¹⁴ relative to the Albright *et al.*¹²⁷ scaled equation of state near the critical temperature, along the critical isochore. The solid line shows deviations for thermal conductivity and the dashed line shows deviations for thermal diffusivity. Deviations for measured thermal diffusivity data are shown with symbols: Δ , Swinney and Henry;¹²⁸ \bullet , Becker and Grigull.⁵²

available. The data at 304.36 K are within 0.2 K of the critical temperature and were not included in the primary data set, while the thermal-conductivity data of Michels *et al.*³⁹ near 305.25 and 307.90 K were used with ξ and C_p from the Span and Wagner¹¹⁴ equation of state. Errors in λ and α due to unphysical behavior of the Span and Wagner equation of state in the critical region are less than 3% and 5%, respectively, near 305.25 K, and 2% and 3%, respectively, near 307.90 K. The largest errors are near the critical density, with systematic deviations in terms of density. The systematic errors in the Span and Wagner¹¹⁴ equation of state contribute to increased deviations for the Michels *et al.*³⁹ data at 305.25 and 307.9 K in Figs. 6 and 7 on the supercritical isotherms, and similarly for the near-critical liquid and vapor in Figs. 10 and 11 and Figs. 4 and 5, respectively.

Figure 22 shows the deviations between the correlation developed here when the equation of state of Span and Wagner¹¹⁴ is used along the critical isochore relative to the same correlation with the scaled equation of state of Albright *et al.*¹²⁷ These deviations represent the maximum deviation observed at any given temperature in the critical

TABLE 7. Sample points for computer verification of the correlating equations

T (K)	ρ (kg m ⁻³)	λ (mW m ⁻¹ K ⁻¹)
250.0	0.0	12.99
250.0	2.0	13.05
250.0	1058.0	140.00
310.0	400.0	73.04 ^a
310.0	400.0	72.28 ^b
310.0	400.0	76.05 ^c
310.0	400.0	39.92 ^d

^aComputed with modified Olchow-Sengers critical enhancement; the viscosity at this point for use in Eq. (5) was taken as $\eta = 28.048$ μ Pa s from Ref. 125 (see Sec. 3.3.1). Thermodynamic properties required for the enhancement term, Eqs. (5)–(8), are from Span and Wagner.¹¹⁴

^bComputed with modified Olchow-Sengers critical enhancement; the viscosity at this point for use in Eq. (5) was taken as $\eta = 28.706$ μ Pa s from Ref. 124. Thermodynamic properties required for the enhancement term, Eqs. (5)–(8), are from Span and Wagner.¹¹⁴

^cComputed with empirical critical enhancement Eq. (10).

^dComputed without any critical enhancement term.

region and increase dramatically as the critical temperature is approached. The thermal diffusivity is overestimated by about 65% with $(T - T_c) = 0.01$ K, while the thermal conductivity is underestimated by about 35% when the Span and Wagner¹¹⁴ equation of state is used. Deviations between the available thermal diffusivity data and the correlation with thermodynamic properties from the scaled equation of state of Albright *et al.*¹²⁷ are also shown for reference. Clearly, the scaled equation of state of Albright *et al.*¹²⁷ should be used at temperatures very close to the critical temperature, when $|(T - T_c)| < 1$ K.

5. Computer-Program Verification and Recommended Values

Table 7 is provided to assist the user in computer-program verification. The thermal-conductivity calculations are based on the tabulated temperatures and densities. Note that the point at 310 K has a very significant contribution from the enhancement term—approximately half of the thermal conductivity is the result of the enhancement term. Table 8 provides some recommended values over the thermal-conductivity surface. Finally, Fig. 23 shows the thermal conductivity of CO₂ as a

TABLE 8. Recommended values of CO₂ thermal conductivity (mW m⁻¹ K⁻¹)

Pressure (MPa)	Temperature (K)									
	240	300	400	500	600	700	800	900	1000	1100
0	12.28	16.72	24.67	32.84	40.93	48.80	56.41	63.72	70.75	77.51
0.1	12.34	16.77	24.72	32.88	40.96	48.83	56.44	63.75	70.78	77.53
20	165.5	106.0	47.40	43.17	48.04	54.31	60.97	67.67	74.28	80.74
40	180.2	127.4	75.10	58.84	57.97	61.23	66.04	71.50	77.23	83.05
60	193.1	143.3	92.68	72.94	68.47	69.29	72.34	76.47	81.18	86.17
80	204.7	156.8	106.5	84.55	77.80	77.02	78.85	81.97	85.81	90.06
100	215.5	168.8	118.5	94.66	86.01	84.00	84.96	87.38	90.60	94.27
120	225.7	179.9	129.5	103.9	93.50	90.33	90.56	92.45	95.22	98.49
140		190.3	139.8	112.6	100.5	96.20	95.70	97.12	99.55	102.5
160		200.1	149.5	121.0	107.3	101.8	100.5	101.5	103.6	106.3
180		209.5	158.8	129.2	114.0	107.2	105.1	105.5	107.3	109.8
200		218.7	167.9	137.2	120.6	112.6	109.6	109.5	110.9	113.1

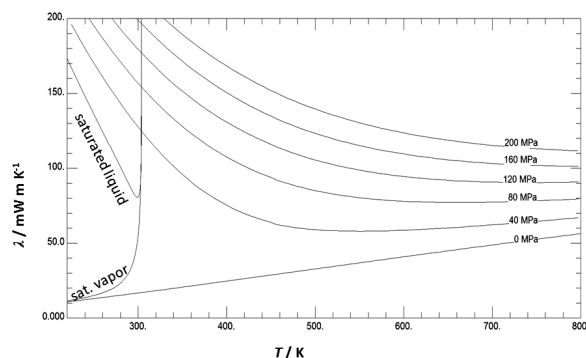


FIG. 23. Thermal conductivity of CO₂ as a function of temperature for different pressures.

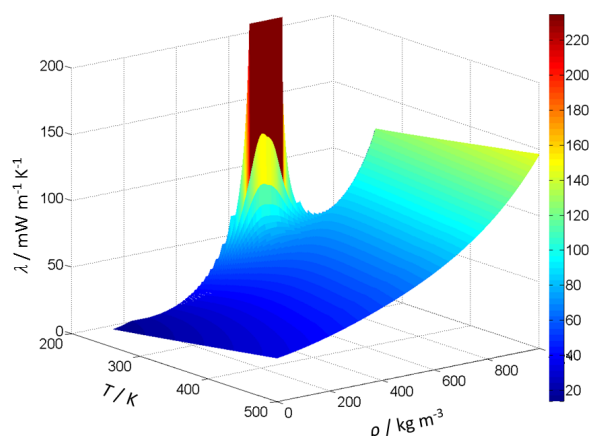


FIG. 24. Thermal-conductivity surface of CO₂.

function of temperature for different pressures calculated with the full model, Eqs. (1) and (3)–(8), while Fig. 24 shows a portion of the three-dimensional thermal conductivity surface, including the critical enhancement, which theoretically approaches infinity at the critical point and has been truncated at 240 mW m^{−1} K^{−1} in this figure.

6. Conclusion

A new wide-ranging correlation for the thermal conductivity of carbon dioxide was developed based on critically evaluated experimental data. The correlation is valid from the triple point to 1100 K, and at pressures up to 200 MPa. The correlation is expressed in terms of temperature and density, and the densities were obtained from the equation of state of Span and Wagner.¹¹⁴ The range of validity of this equation of state is 1100 K and 800 MPa. We recommend the use of the present thermal-conductivity correlation only to 200 MPa, as there were no data available for validation at pressures above 200 MPa. The new formulation incorporates new experimental data of Perkins⁷ in the liquid phase, and recent theoretical calculations of Hellmann⁸ for the dilute-gas region. The overall uncertainty (at the 95% confidence level) of the proposed correlation varies depending on the state point from a low of 1% at very low pressures below 0.1 MPa between 300 and 700 K, to 5% at the higher pressures of the range of validity. Representation of data very near the critical point is adversely

affected by some anomalous behavior of the Span–Wagner¹¹⁴ equation of state; future improvements in the equation of state would permit improvements in the critical region. In addition, there is room for improvement in the high-pressure region (100–200 MPa) due to limited data in this region.

Acknowledgments

Funding for much of this work was provided by the U.S. Department of Energy, National Energy Technology Laboratory, under Interagency Agreement No. DE-FE0003931. We acknowledge David J. N. Wynne (Univ. of Colorado, Boulder) for helpful suggestions.

7. References

- ¹Supercritical Fluid Methods Protocols, edited by J. R. Williams and A. A. Clifford (Humana Press, Totowa, NJ, 2000).
- ²P. K. Bansal, *Appl. Therm. Eng.* **41**, 18 (2012).
- ³National Energy Technology Laboratory, Carbon Dioxide Enhanced Oil Recovery, 2010, http://www.netl.doe.gov/file%20library/research/oil-gas/CO2_EOR_Primer.pdf.
- ⁴New Brayton cycle turbines promise giant leap in performance, Sandia Lab News, 2011, <http://www.sandia.gov/LabNews/110211.html>.
- ⁵V. Vesovic, W. A. Wakeham, G. A. Olchowy, J. V. Sengers, J. T. R. Watson, and J. Millat, *J. Phys. Chem. Ref. Data* **19**, 763 (1990).
- ⁶G. Scalabrin, P. Marchi, F. Finezzo, and R. Span, *J. Phys. Chem. Ref. Data* **35**, 1549 (2006).
- ⁷R. A. Perkins, "Measurement of the thermal conductivity of carbon dioxide at temperatures from the triple point to 756 K with pressures up to 69 MPa," *J. Chem. Eng. Data* (unpublished).
- ⁸R. Hellmann, *Chem. Phys. Lett.* **613**, 133 (2014).
- ⁹M. J. Assael, J. A. M. Assael, M. L. Huber, R. A. Perkins, and Y. Takata, *J. Phys. Chem. Ref. Data* **40**, 033101 (2011).
- ¹⁰M. J. Assael, I. A. Koini, K. D. Antoniadis, M. L. Huber, I. M. Abdulagatov, and R. A. Perkins, *J. Phys. Chem. Ref. Data* **41**, 023104 (2012).
- ¹¹M. J. Assael, S. K. Mylona, M. L. Huber, and R. A. Perkins, *J. Phys. Chem. Ref. Data* **41**, 023101 (2012).
- ¹²M. J. Assael, E. K. Mihailidou, M. L. Huber, R. A. Perkins, and I. M. Abdulagatov, *J. Phys. Chem. Ref. Data* **41**, 043102 (2012).
- ¹³S. K. Mylona, K. D. Antoniadis, M. J. Assael, M. L. Huber, and R. A. Perkins, *J. Phys. Chem. Ref. Data* **43**, 043104 (2014).
- ¹⁴M. J. Assael, S. K. Mylona, M. L. Huber, and R. A. Perkins, *J. Phys. Chem. Ref. Data* **42**, 013106 (2013).
- ¹⁵M. J. Assael, I. Bogdanou, S. K. Mylona, M. L. Huber, R. A. Perkins, and V. Vesovic, *J. Phys. Chem. Ref. Data* **42**, 023101 (2013).
- ¹⁶E. A. Sykioti, M. J. Assael, M. L. Huber, and R. A. Perkins, *J. Phys. Chem. Ref. Data* **42**, 043101 (2013).
- ¹⁷M. J. Assael, E. A. Sykioti, M. L. Huber, and R. A. Perkins, *J. Phys. Chem. Ref. Data* **42**, 023102 (2013).
- ¹⁸M. L. Huber, R. A. Perkins, D. G. Friend, J. V. Sengers, M. J. Assael, I. N. Metaxa, K. Miyagawa, R. Hellmann, and E. Vogel, *J. Phys. Chem. Ref. Data* **41**, 033102 (2012).
- ¹⁹E. K. Michailidou, M. J. Assael, M. L. Huber, and R. A. Perkins, *J. Phys. Chem. Ref. Data* **42**, 033104 (2013).
- ²⁰E. K. Michailidou, M. J. Assael, M. L. Huber, I. M. Abdulagatov, and R. A. Perkins, *J. Phys. Chem. Ref. Data* **43**, 023103 (2014).
- ²¹M. L. Huber, R. A. Perkins, A. Laesecke, D. G. Friend, J. V. Sengers, M. J. Assael, I. N. Metaxa, E. Vogel, R. Mares, and K. Miyagawa, *J. Phys. Chem. Ref. Data* **38**, 101 (2009).
- ²²S. Avgeri, M. J. Assael, M. L. Huber, and R. A. Perkins, *J. Phys. Chem. Ref. Data* **43**, 033103 (2014).
- ²³M. J. Assael, M. L. V. Ramires, C. A. Nieto de Castro, and W. A. Wakeham, *J. Phys. Chem. Ref. Data* **19**, 113 (1990).
- ²⁴S. F. Y. Li, M. Papadaki, and W. A. Wakeham, "Thermal conductivity of low density polyatomic gases," *Proceedings of the 22nd International Conference on Thermal Conductivity*, edited by T. W. Tong (Technomic Publishing Company, Lancaster, PA, 1994), p. 531.

- ²⁵J. Millat, M. Mustafa, M. Ross, W. A. Wakeham, and M. Zalaf, *Physica A* **145**, 461 (1987).
- ²⁶A. I. Johns, S. Rashid, and J. T. R. Watson, *J. Chem. Soc., Faraday Trans. 1* **82**, 2235 (1986).
- ²⁷N. Imaishi, J. Kestin, and W. A. Wakeham, *Physica A* **123**, 50 (1984).
- ²⁸A. C. Scott, A. I. Johns, J. T. R. Watson, and A. A. Clifford, *J. Chem. Soc., Faraday Trans. 1* **79**, 733 (1983).
- ²⁹A. A. Clifford, J. Kestin, and W. A. Wakeham, *Physica A* **97**, 287 (1979).
- ³⁰J. A. A. Snel, N. J. Trappeniers, and A. Botzen, *Proc. K. Ned. Akad. Wet., Ser. B* **82**, 316 (1979).
- ³¹A. A. Tarzimanov and V. A. Arslanov, *Teploni Mass. V Khim. Tekhnol.* **3**, 13 (1978).
- ³²S. S. Bakulin, S. A. Ulybin, and E. P. Zherdev, *High Temp.* **14**, 351 (1976).
- ³³S. S. Bakulin, S. A. Ulybin, and E. P. Zherdev, *Teplofiz. Vys. Temp.* **13**, 96 (1975).
- ³⁴J. W. Haarman, *AIP Conf. Proc.* **11**, 193 (1973).
- ³⁵B. Le Neindre, R. Tufeu, P. Bury, and J. V. Sengers, *Ber. Bunsen-Ges. Phys. Chem.* **77**, 262 (1973).
- ³⁶B. Le Neindre, P. Bury, R. Tufeu, P. Johannin, and B. Vodar, presented at the Ninth Conference on Thermal Conductivity, Iowa State University, Ames, Iowa, 1969.
- ³⁷B. Le Neindre, *Int. J. Heat Mass Transfer* **15**, 1 (1972).
- ³⁸B. Le Neindre, P. Bury, R. Tufeu, P. Johannin, and B. Vodar, *Proceedings of the 7th Conference on Thermal Conductivity* (National Bureau of Standards, Washington, DC, 1968), Vol. 7, p. 579.
- ³⁹A. Michels, J. V. Sengers, and P. S. Van der Gulik, *Physica* **28**, 1216 (1962).
- ⁴⁰F. G. Keyes, *Trans. ASME* **77**, 1395 (1955).
- ⁴¹F. G. Keyes, *Trans. ASME* **73**, 597 (1951).
- ⁴²J. M. Lenoir and E. W. Comings, *Chem. Eng. Prog.* **47**, 223 (1951).
- ⁴³H. L. Johnston and E. R. Grilly, *J. Chem. Phys.* **14**, 233 (1946).
- ⁴⁴B. G. Dickins, *Proc. R. Soc. A* **143**, 517 (1934).
- ⁴⁵D. Tomida, T. Odashima, and C. Yokohama, *Kagaku Kogaku Ronbunshu* **36**, 429 (2010).
- ⁴⁶J. Patek, J. Klomfar, L. Capla, and P. Buryan, *Int. J. Thermophys.* **26**, 577 (2005).
- ⁴⁷T. Heinemann, W. Klaen, R. Yourd, and R. Dohrn, *J. Cell. Plast.* **36**, 45 (2000).
- ⁴⁸Z.-H. Chen, K.-I. Tozaki, and K. Nishikawa, *Jpn. J. Appl. Phys., Part 1* **38**, 6840 (1999).
- ⁴⁹R. Dohrn, R. Treckmann, and T. Heinemann, *Fluid Phase Equilib.* **158-160**, 1021 (1999).
- ⁵⁰X.-Y. Zheng, S. Yamamoto, H. Yoshida, H. Masuoka, and M. Yorizane, *J. Chem. Eng. Jpn.* **17**, 237 (1984).
- ⁵¹M. Yorizane, S. Yoshimura, H. Masuoka, and H. Yoshida, *Ind. Eng. Chem. Fundam.* **22**, 454 (1983).
- ⁵²H. Becker and U. Grigull, *Wärme- Stoffübertragung* **11**, 9 (1978).
- ⁵³S. A. Ulybin and S. S. Bakulin, *Teplenergetika* **24**, 85 (1977).
- ⁵⁴S. H. P. Chen, P. C. Jain, and S. C. Saxena, *J. Phys. B* **8**, 1962 (1975).
- ⁵⁵R. S. Salmanov and A. A. Tarzimanov, *Trudy Kazanskogo Khim.-Tekhnol. Inst. im. Kirova* **51**, 161 (1973).
- ⁵⁶A. G. Shashkov and F. P. Kamchatov, *Vesti Akad. Nauka BSSR, Ser. Fiz. Energ. Navuk* **3**, 61 (1973).
- ⁵⁷K. M. Dijkema, J. C. Stouthart, and D. A. De Vries, *Wärme-Stoffübertragung* **5**, 47 (1972).
- ⁵⁸G. P. Gupta and S. C. Saxena, *Mol. Phys.* **19**, 871 (1970).
- ⁵⁹A. O. S. Maczek and P. Gray, *Trans. Faraday Soc.* **66**, 127 (1970).
- ⁶⁰M. L. R. Murthy and H. A. Simon, presented at the Fifth Symposium on Thermophysical Properties, Newton, MA, 1970.
- ⁶¹M. L. R. Murthy and H. A. Simon, *Phys. Rev. A* **2**, 1458 (1970).
- ⁶²A. A. Tarzimanov, *Trudy Kazanskogo Khim.-Tekhnol. Inst. im. Kirova* **45**, 235 (1970).
- ⁶³I. F. Golubev and V. P. Kiyashova, "Chemistry and technology of nitrogen fertilizer and organic synthesis products," *Phys.-Chem. Stud.* **70** (1969).
- ⁶⁴B. M. Rosenbaum and G. Thodos, *J. Chem. Phys.* **51**, 1361 (1969).
- ⁶⁵A. K. Barua, A. Manna, and P. Mukhopadhyay, *J. Phys. Soc. Jpn.* **25**, 862 (1968).
- ⁶⁶R. V. Shingarev, "Table 10.2," in *Thermophysical Properties of CO₂*, edited by M. P. Vukalovich and V. A. Altunin (Collets, London, 1968).
- ⁶⁷W. Van Dael and H. Cauwenbergh, *Physica* **40**, 165 (1968).
- ⁶⁸P. J. Freud and G. M. Rothberg, *Rev. Sci. Instrum.* **38**, 238 (1967).
- ⁶⁹P. Mukhopadhyay, A. Das Gupta, and A. K. Barua, *Br. J. Appl. Phys.* **18**, 1301 (1967).
- ⁷⁰P. Mukhopadhyay and A. K. Barua, *Trans. Faraday Soc.* **63**, 2379 (1967).
- ⁷¹C. E. Baker and R. S. Brokaw, *J. Chem. Phys.* **40**, 1523 (1964).
- ⁷²H. Senftleben, *Z. Angew. Phys.* **17**, 86 (1964).
- ⁷³K. I. Amirkhanov and A. P. Adamov, *Teplenergetika* **10**, 77 (1963).
- ⁷⁴H. Cheung, L. A. Bromley, and C. R. Wilke, *AIChE J.* **8**, 221 (1962).
- ⁷⁵L. A. Guildner, *J. Res. Natl. Bur. Stand., Sect. A* **66A**, 341 (1962).
- ⁷⁶A. A. Westenberg and N. DeHaas, *Phys. Fluids* **5**, 266 (1962).
- ⁷⁷H. Geier and K. Schafer, *Allg. Warmetechnik* **10**, 70 (1961).
- ⁷⁸R. G. Vines, *Trans. ASME* **82**, 48 (1960).
- ⁷⁹A. M. Chaikin and A. M. Markevich, *Zh. Fiz. Khim.* **32**, 116 (1958).
- ⁸⁰L. A. Guildner, *Proc. Natl. Acad. Sci. U. S. A.* **44**, 1149 (1958).
- ⁸¹F. G. Waelbroeck and P. Zuckerbrodt, *J. Chem. Phys.* **28**, 523 (1958).
- ⁸²C. Salceanu and S. Bojin, *Compt. Rend.* **243**, 237 (1956).
- ⁸³I. A. Kulakov, *Izv. Voronezh Pedagog. Inst.* **17**, 85 (1955).
- ⁸⁴A. J. Rothman and L. A. Bromley, *Ind. Eng. Chem.* **47**, 899 (1955).
- ⁸⁵L. P. Filippov, *Vestnik Moskov. Univ.* **12**, 45 (1954).
- ⁸⁶L. B. Thomas and R. C. Golike, *J. Chem. Phys.* **22**, 300 (1954).
- ⁸⁷J. M. Davidson and J. F. Music, *Experimental Thermal Conductivities of Gases and Gaseous Mixtures at Zero Degrees Centigrade* (Hanford Atomic Products Operation, Richland, WA, 1953).
- ⁸⁸A. J. Rothman, "Thermal conductivity of gases at high temperatures," US Atomic Energy Commission Report UCRL-2339, 1953.
- ⁸⁹E. U. Franck, *Z. Elektrochem.* **55**, 636 (1951).
- ⁹⁰W. G. Kannuliuk and H. B. Donald, *Aust. J. Sci. Res., Ser. A* **3**, 417 (1950).
- ⁹¹E. A. Stolyarov, V. V. Ipatjer, and V. P. Theodorowitsch, *Zh. Fiz. Khim.* **24**, 166 (1950).
- ⁹²E. Borovik, *Zh. Eksper. Teor. Fiz.* **19**, 561 (1949).
- ⁹³F. G. Keyes, "Summary of measurements of heat conductivity carried out under the Office of Naval Research Program from 1 July 1947 to 15 June 1949," Report on Project NR-058-037, 1949.
- ⁹⁴D. W. Stops, *Nature* **164**, 966 (1949).
- ⁹⁵D. L. Timrot and V. G. Oskolkova, *Izvestiya VTI* **18**, 4 (1949).
- ⁹⁶W. G. Kannuliuk and P. G. Law, *Proc. R. Soc. Victoria* **58**, 142 (1947).
- ⁹⁷N. B. Vargaftik and O. N. Oleshuk, *Izv. Vses. Teplotekhn. Inst. Feliksn Dzerzhinskogo* **15**, 7 (1946).
- ⁹⁸A. Eucken, *Forsch. Geb. Ingenieurwes.* **11**, 6 (1940).
- ⁹⁹B. Koch and W. Fritz, *Wärme und Kältetechnik Zeitschrift für Klimatechnik, Trockentechnik Wärme und Schallschutztechnik* **42**, 113 (1940).
- ¹⁰⁰G. G. Sherratt and E. Griffiths, *Philos. Mag.* **27**, 68 (1939).
- ¹⁰¹C. T. Archer, *Philos. Mag.* **19**, 901 (1935).
- ¹⁰²W. G. Kannuliuk and L. H. Martin, *Proc. R. Soc. A* **144**, 496 (1934).
- ¹⁰³A. Kardos, *Z. Ges. Kalte Ind.* **41**, 1 (1934).
- ¹⁰⁴W. Sellschopp, *Forsch. Geb. Ingenieurwes.* **5**, 162 (1934).
- ¹⁰⁵M. Trautz and A. Zundel, *Ann. Phys.* **17**, 345 (1933).
- ¹⁰⁶G. Kornfeld and K. Hilferding, *Bodenstein-Festband* **792** (1931).
- ¹⁰⁷H. Gregory and S. Marshall, *Proc. R. Soc. A* **114**, 354 (1927).
- ¹⁰⁸S. Weber, *Ann. Phys.* **82**, 479 (1927).
- ¹⁰⁹S. Weber, *Ann. Phys.* **54**, 437 (1917).
- ¹¹⁰A. Schleiermacher, *Ann. Phys. Chem.* **270**, 623 (1888).
- ¹¹¹L. Graetz, *Ann. Phys. Chem.* **14**, 232 (1881).
- ¹¹²A. Winkelmann, *Ann. Phys.* **11**, 474 (1880).
- ¹¹³H. Preston-Thomas, *Metrologia* **27**, 3 (1990).
- ¹¹⁴R. Span and W. Wagner, *J. Phys. Chem. Ref. Data* **25**, 1509 (1996).
- ¹¹⁵M. G. Cox, *Metrologia* **39**, 589 (2002).
- ¹¹⁶P. T. Boggs, R. H. Byrd, J. E. Rogers, and R. B. Schnabel, *ODRPACK*, Software for Orthogonal Distance Regression, NISTIR 4834, v2.013, National Institute of Standards and Technology, Gaithersburg, MD, 1992.
- ¹¹⁷N. B. Vargaftik, *Handbook of Physical Properties of Liquids and Gases: Pure Substances and Mixtures* (Hemisphere Publishing Corporation, New York, 1983).
- ¹¹⁸G. A. Olchoway and J. V. Sengers, *Phys. Rev. Lett.* **61**, 15 (1988).
- ¹¹⁹R. Mostert, H. R. van den berg, P. S. Van der Gulik, and J. V. Sengers, *J. Chem. Phys.* **92**, 5454 (1990).
- ¹²⁰R. A. Perkins, H. M. Roder, D. G. Friend, and C. A. Nieto de Castro, *Physica* **173**, 332 (1991).
- ¹²¹R. A. Perkins, J. V. Sengers, I. M. Abdulagatov, and M. L. Huber, *Int. J. Thermophys.* **34**, 191 (2013).
- ¹²²J. V. Sengers and R. A. Perkins, "Fluids near critical points," in *Experimental Thermodynamics Volume IX: Advances in Transport Properties of*

- Fluids*, edited by A. R. H. Goodwin, M. J. Assael, V. Vesovic, and W. A. Wakeham (Royal Society of Chemistry, Cambridge, 2014), Chap. 10, pp. 337–361.
- ¹²³G. A. Olchoway and J. V. Sengers, *Int. J. Thermophys.* **10**, 417 (1989).
- ¹²⁴A. Fenghour, W. A. Wakeham, and V. Vesovic, *J. Phys. Chem. Ref. Data* **27**, 31 (1998).
- ¹²⁵A. Laesecke and C. D. Muzny, “Reference Correlation of the Viscosity of CO₂,” *J. Phys. Chem. Ref. Data* (unpublished).
- ¹²⁶E. W. Lemmon, M. L. Huber, and M. O. McLinden, NIST Standard Reference Database 23, NIST Reference Fluid Thermodynamic and Transport Properties Database (REFPROP), version 9.1, National Institute of Standards and Technology, Gaithersburg, MD, 2013.
- ¹²⁷P. C. Albright, T. J. Edwards, Z. Y. Chen, and J. V. Sengers, *J. Chem. Phys.* **87**, 1717 (1987).
- ¹²⁸H. L. Swinney and D. L. Henry, *Phys. Rev. A* **8**, 2586 (1973).
- ¹²⁹Y. Garrabos, R. Tufeu, B. LeNeindre, G. Zalczer, and D. Beysens, *J. Chem. Phys.* **72**, 4637 (1980).
- ¹³⁰E. Reile, P. Jany, and J. Straub, *Wärme Stoffübertragung* **18**, 99 (1984).
- ¹³¹B. S. Maccabee and J. A. White, *Phys. Lett. A* **35**, 187 (1971).
- ¹³²K. Kawasaki, *Phys. Rev. A* **1**, 1750 (1970).
- ¹³³D. L. Henry, H. L. Swinney, and H. Z. Cummins, *Phys. Rev. Lett.* **25**, 1170 (1970).
- ¹³⁴EUREQA Formulize v.098.1, Nutonian, Inc., MA, USA. Certain commercial products are identified in this paper to adequately specify the procedures used. Such identification does not imply recommendation or endorsement by the National Institute of Standards and Technology nor does it imply that the products identified are necessarily the best available for that purpose.